Partial Differential Equations, Optimal Control, and Numerics

Simulation of Resistivity and Sonic Borehole Logging Measurements Using hp Finite Elements

D. Pardo, P. Matuszyk, M.J. Nam, C. Torres-Verdín, V. M. Calo

Basque Center for Applied Mathematics (BCAM)

TEAM MEMBERS:
D. Pardo (Research Professor)
I. Garay (Postdoctoral Fellow)
A.-G. Saint-Guirons (Postdoctoral Fellow)
I. Andonegui (Technician)

MAIN COLLABORATORS:
M. J. Nam, F. de la Hoz
M. Paszynski, L.E. García-Castillo
I. Gómez, C. Torres-Verdín
P. Matuszyk, L. Demkowicz

1 Sep. 2009

overview

1. Motivation.
2. Method.
3. Sonic Simulations.
4. Electromagnetic Simulations.
5. Inverse Problems.
6. Conclusions.

motivation and objectives

Multiphysics Logging Measurements

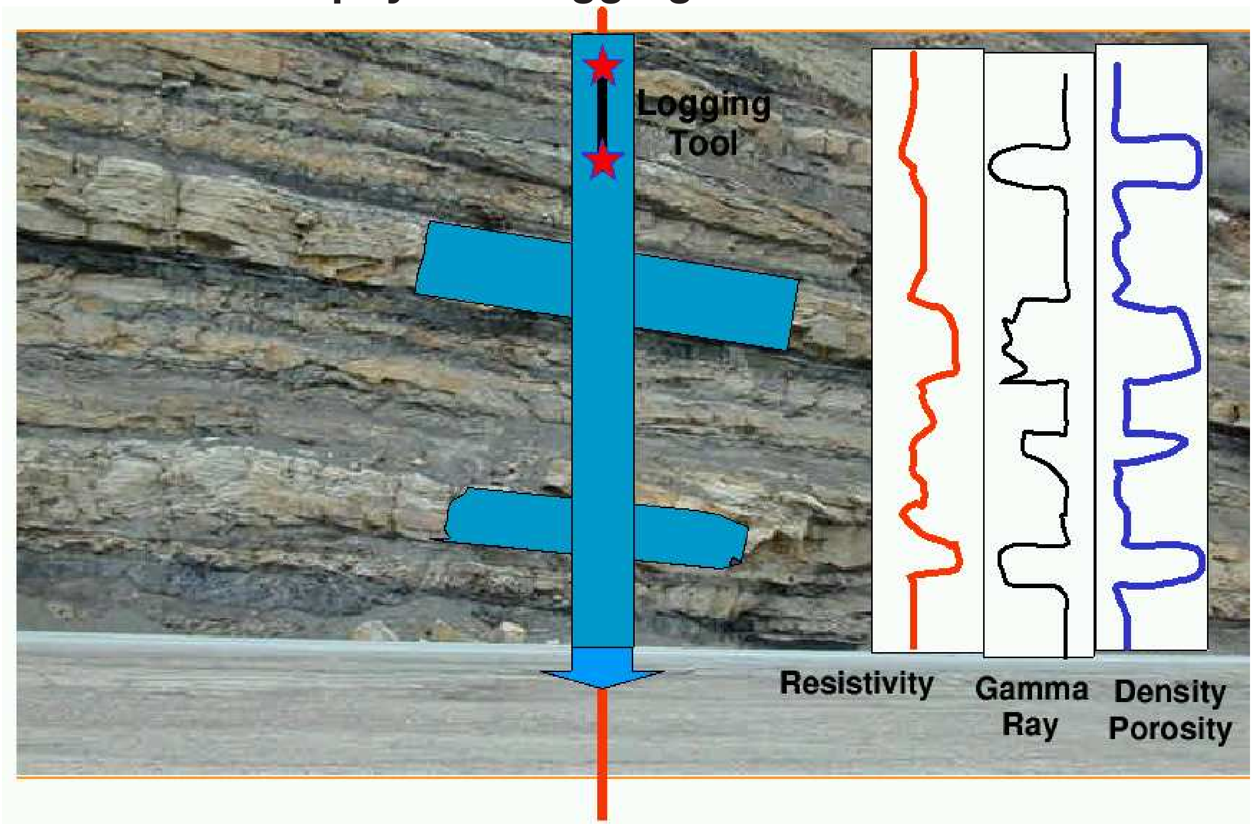

OBJECTIVES: To determine payzones (porosity), amount of oil/gas (saturation), and ability to extract oil/gas (permeability).

motivation and objectives

Main Objective: To Solve a Multiphysics Inverse Problem

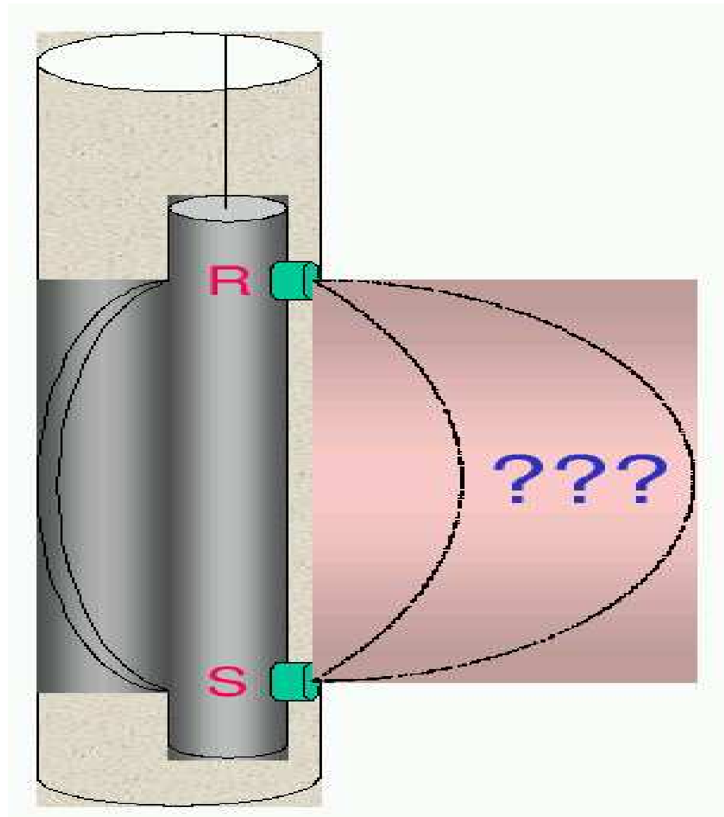

Software to solve the DIRECT problem is essential in order to solve the INVERSE problem.

method

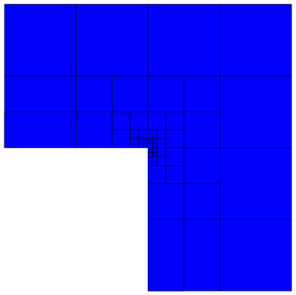

The h-Finite Element Method

1. Convergence limited by the polynomial degree, and large material contrasts.
2. Optimal h-grids do NOT converge exponentially in real applications.
3. They may "lock" (100$\%$ error).

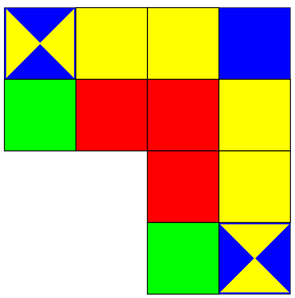

The p-Finite Element Method

1. Exponential convergence feasible for analytical ("nice") solutions.
2. Optimal *p*-grids do NOT converge exponentially in real applications.
3. If initial *h*-grid is not adequate, the *p*-method will fail miserably.

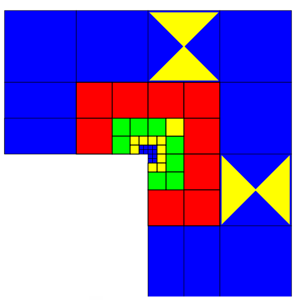

The hp-Finite Element Method

1. Exponential convergence feasible for ALL solutions.
2. Optimal *hp*-grids DO converge exponentially in real applications.
3. If initial *hp*-grid is not adequate, results will still be great.

method

Energy norm based fully automatic *hp*-adaptive strategy

Coarse grids (hp) **Fine grids** $(h/2, p+1)$

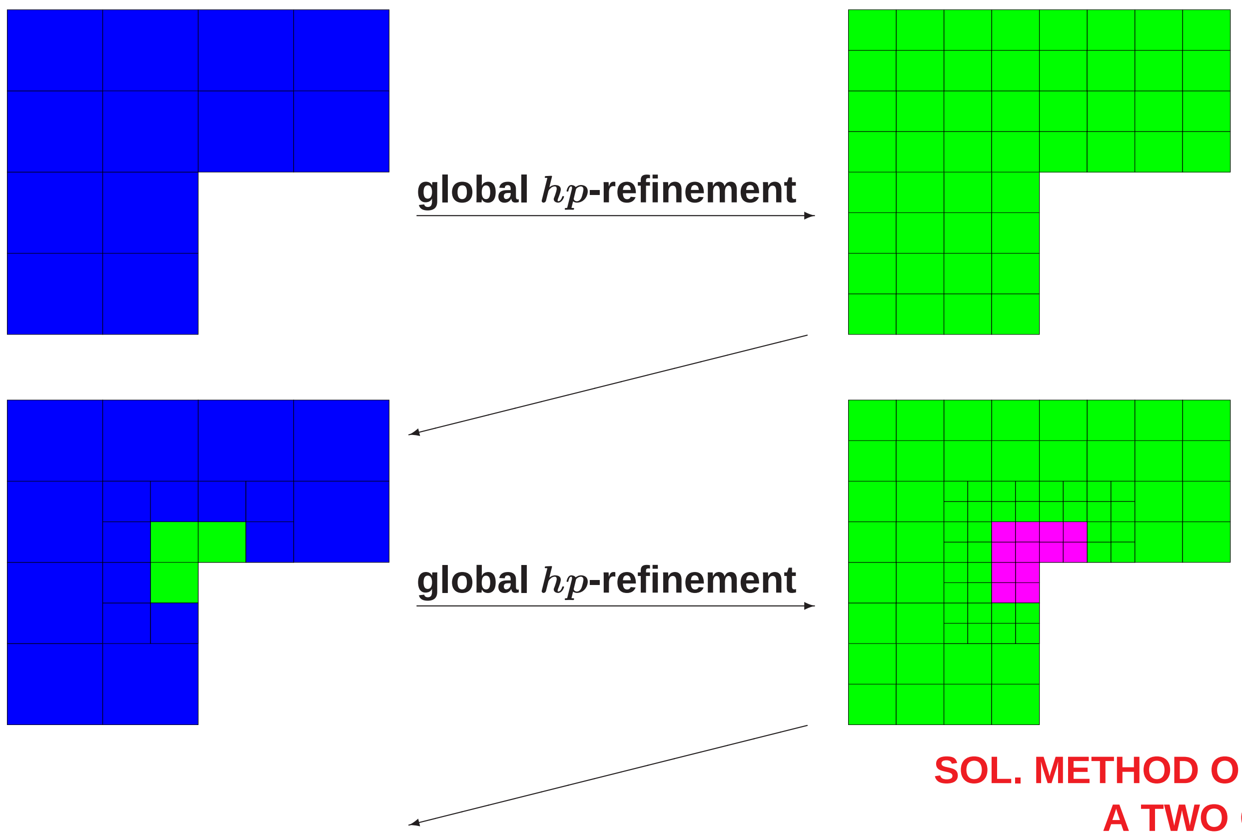

SOL. METHOD ON FINE GRIDS: A TWO GRID SOLVER

method

Refinement strategy

Notation:

- K is an element of the hp-grid.
- $E_C = E_{hp}$ (coarse grid) $\prec$ $E_{\widehat{hp}}$ $\prec$ $E_F = E_{h/2,p+1}$ (fine grid).

The adaptive strategy maximizes the following quantity:

$$\widehat{hp} = arg \max_{\widetilde{hp}} \sum_K \frac{|E_F - \Pi^K_{hp} E_F|^2_{?,K} - |E_F - \Pi^K_{\widetilde{hp}} E_F|^2_{?,K}}{(N_{\widetilde{hp}} - N_{hp})^2},$$

where $\Pi^K_{hp} E_F$ is the projection based interpolation of solution E_F over the K-th element of the hp grid.

The choice of the semi-norm depends upon the space in which the solution lives —H^1, $H(\mathrm{curl})$, $H(div)$ or L^2—.

method

Projection based interpolation

$$\Pi_{hp}^{K} E_F = E_1^{K,hp} + E_2^{K,hp} + E_3^{K,hp}.$$

- $E_1^{K,hp}$ **is the "bilinear vertex interpolant" of the** K**-th element of the** hp**-grid.**
- $E_2^{K,hp}$ **is the "projection" of** $E_F - E_1^{K,hp}$ **over each edge of the** K**-th element of the** hp**-grid.**
- $E_3^{K,hp}$ **is the "projection" of** $E_F - E_1^{K,hp} - E_2^{K,hp}$ **over the interior of the** K**-th element of the** hp**-grid.**

The projection depends upon the space in which the solution lives —H^1**,** $H(\mathrm{curl})$**,** $H(div)$ **or** L^2**—.**

Question: How can we combine energies coming from different norms/spaces?

method

De Rham diagram

De Rham diagram is critical to the theory of FE discretizations of multi-physics problems.

$$
\begin{tikzcd}
\mathbb{R} \arrow[r] \arrow[d, "id"] & W \arrow[r, "\nabla"] \arrow[d, "\Pi"] & Q \arrow[r, "\nabla\times"] \arrow[d, "\Pi^{\mathrm{curl}}"] & V \arrow[r, "\nabla\circ"] \arrow[d, "\Pi^{\mathrm{div}}"] & L^2 \arrow[r] \arrow[d, "P"] & 0 \\
\mathbb{R} \arrow[r] & W^{\mathrm{p}} \arrow[r, "\nabla"] & \mathrm{Q}^{\mathrm{p}} \arrow[r, "\nabla\times"] & \mathrm{V}^{\mathrm{p}} \arrow[r, "\nabla\circ"] & W^{\mathrm{p}-1} \arrow[r] & 0 \,.
\end{tikzcd}
$$

This diagram relates two exact sequences of spaces, on both continuous and discrete levels, and corresponding interpolation operators.

method

Mathematical Formulation (Goal-Oriented Adaptivity)

We consider the following problem (in variational form):

$$\begin{cases} \text{Find } L(E)\text{, where } E \in V \text{ such that :} \\ b(E,\xi) = f(\xi) \quad \forall \xi \in V \ . \end{cases}$$

We define residual $r_e(\xi) = b(e,\xi)$. We seek for solution G of:

$$\begin{cases} \text{Find } G \in V'' \sim V \text{ such that :} \\ G(r_e) = L(e) \ . \end{cases}$$

This is necessarily solved if we find the solution of the *dual* problem:

$$\begin{cases} \text{Find } G \in V \text{ such that :} \\ b(E,G) = L(E) \quad \forall E \in V \ . \end{cases}$$

Notice that $L(e) = b(e,G)$.

method

Algorithm for Goal-Oriented Adaptivity

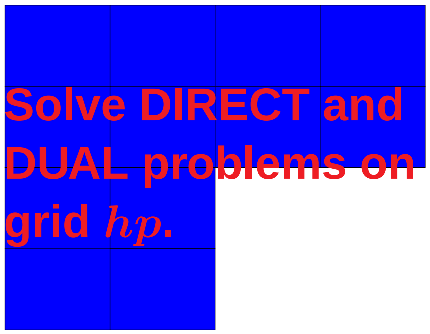

$\longrightarrow$

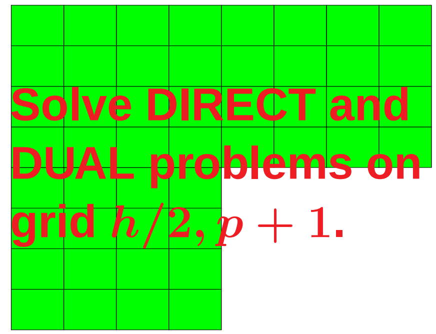

Compute $e = E_{h/2,p+1} - E_{hp}$, and $\epsilon = G_{h/2,p+1} - G_{hp}$.
Represent the error as: $|L(e)| = |b(e,\epsilon)| \leq \sum_K |b_K(e,\epsilon)|$.
Apply the fully automatic hp-adaptive algorithm.

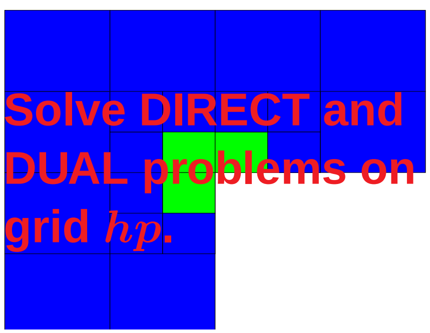

$\longrightarrow$

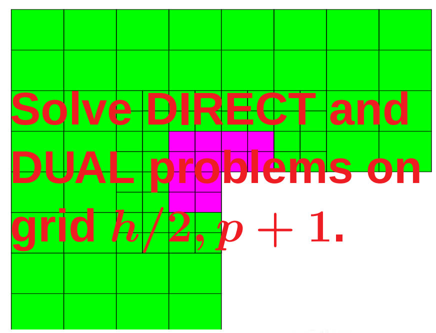

sonic simulations

- **Acoustic domain: borehole fluid (c_f, ρ_f)**

$$\begin{cases} i\omega p + c_f^2 \rho_f \nabla \cdot v = 0 \\ i\omega \rho_f v + \nabla p = 0 \end{cases}$$

- **Elastic tool, casing, formation (V_p, V_s, ρ_s)**

$$0 = \nabla \cdot \sigma + \rho_s \omega^2 u$$
$$\sigma = \lambda I \nabla \cdot u + \mu(\nabla u + \nabla^T u)$$
$$\lambda = \rho_s (V_p^2 - 2V_s^2), \ \mu = \rho_s V_s^2$$

- **Coupling:**

$$n_f \cdot \nabla p = \rho_f \omega^2 n_f \cdot u$$
$$n_s \cdot \sigma = -p n_s$$

- **Acoustic source:**

$$n_f \cdot \nabla p = 1$$

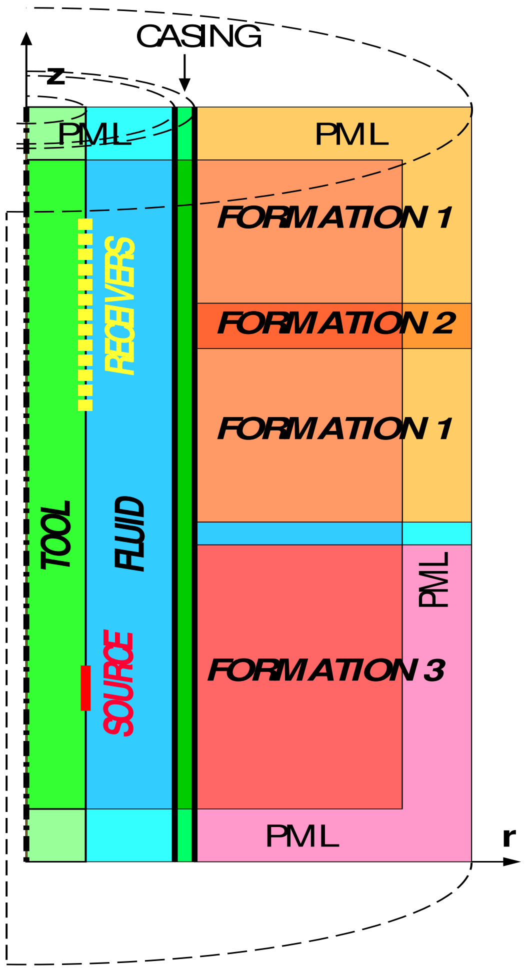

sonic simulations

Verification of Sonic Measurements

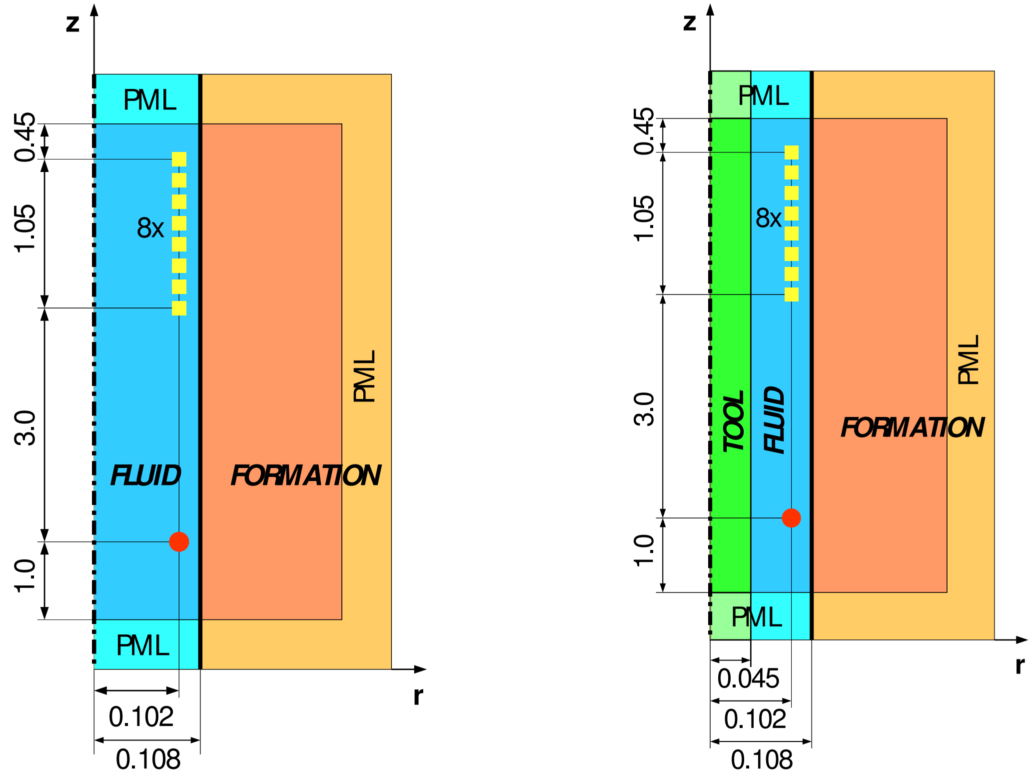

- **Formation thickness: 0.25m.**
- **Monopole and dipole source, central frequency 8603 Hz.**

sonic simulations

Monopole source — fast formation

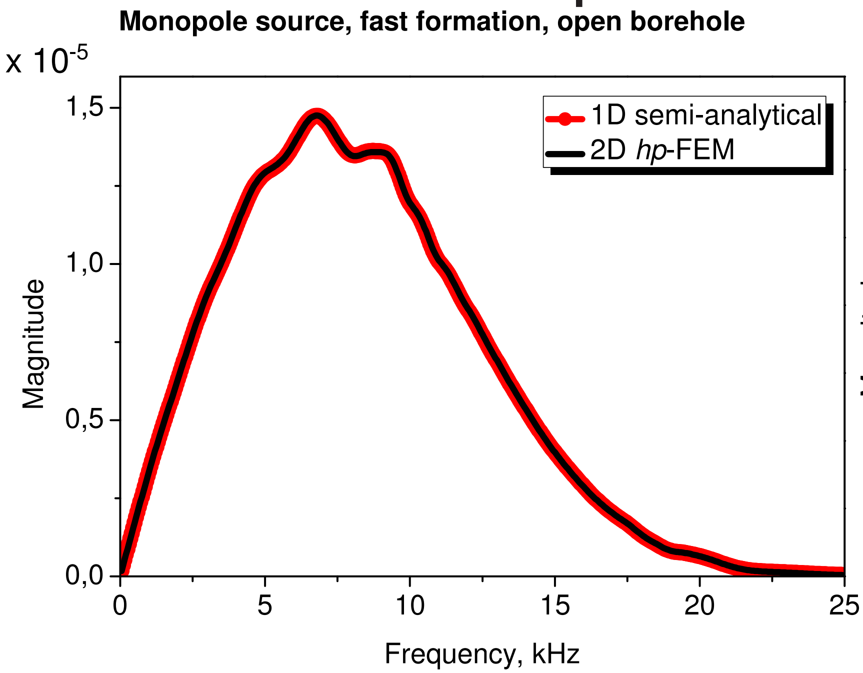

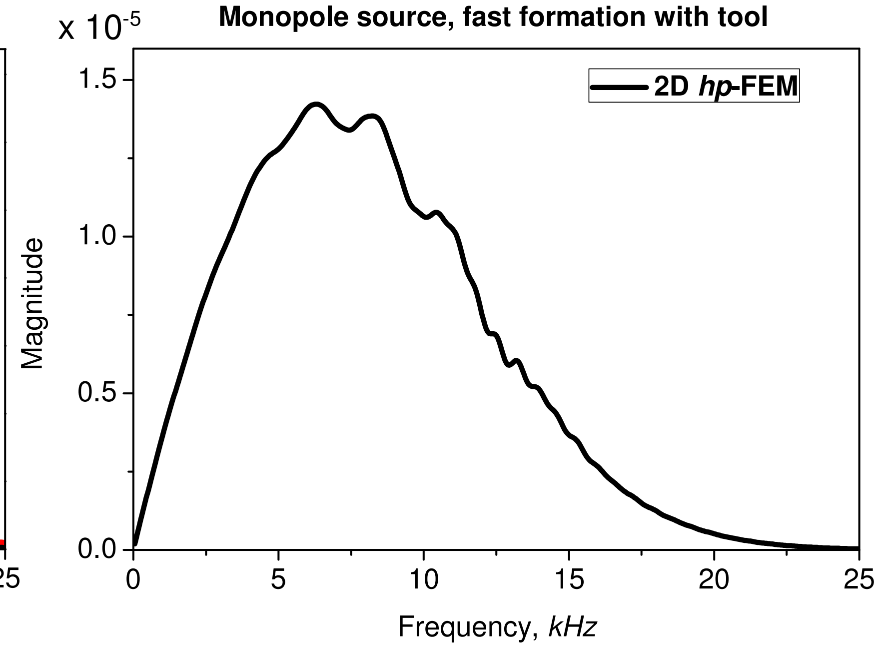

	P-wave		S-wave		Density
	$V_p\ [m/s]$	$1/V_p\ [\mu s/ft]$	$V_s\ [m/s]$	$1/V_s\ [\mu s/ft]$	$\rho\ [kg/m^3]$
fluid	1524	200.0	–	–	1100
fast form.	3048	100.0	1793	170.0	2200
tool	5860	52.0	3130	97.4	7800

www.bcamath.org
basque center for applied mathematics

sonic simulations

Monopole source — fast formation — no tool

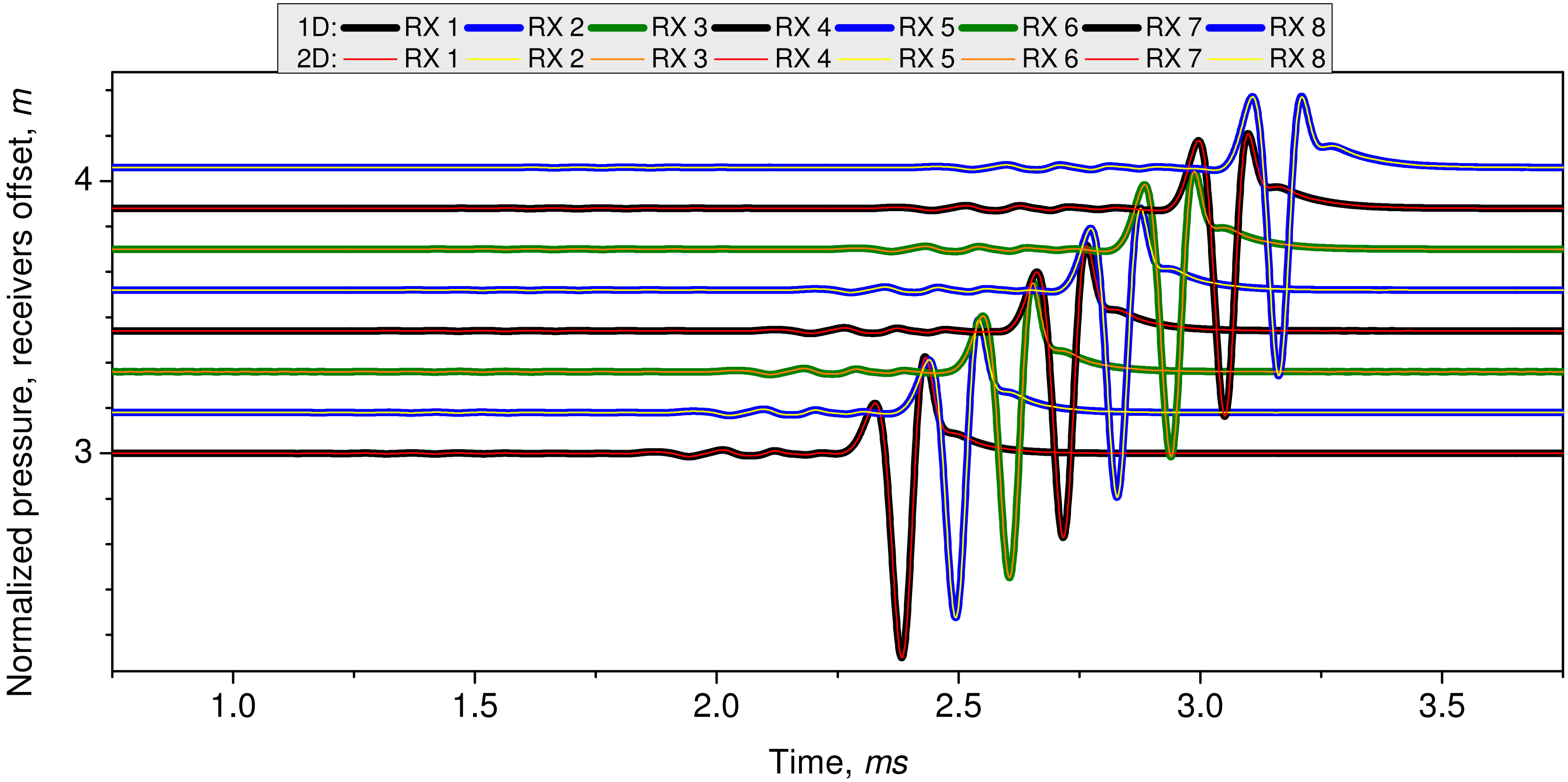

sonic simulations

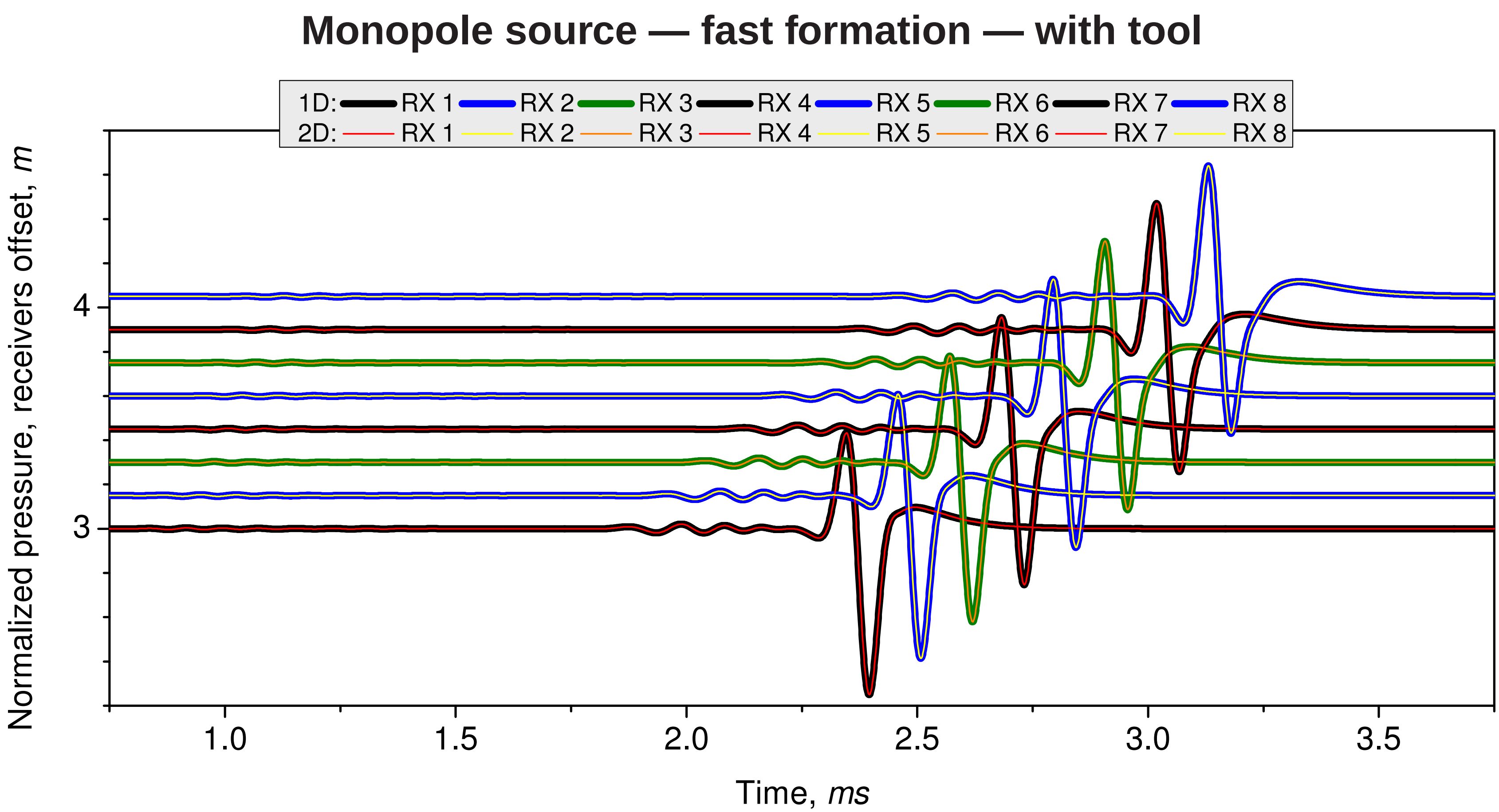

sonic simulations

Monopole source — fast formation

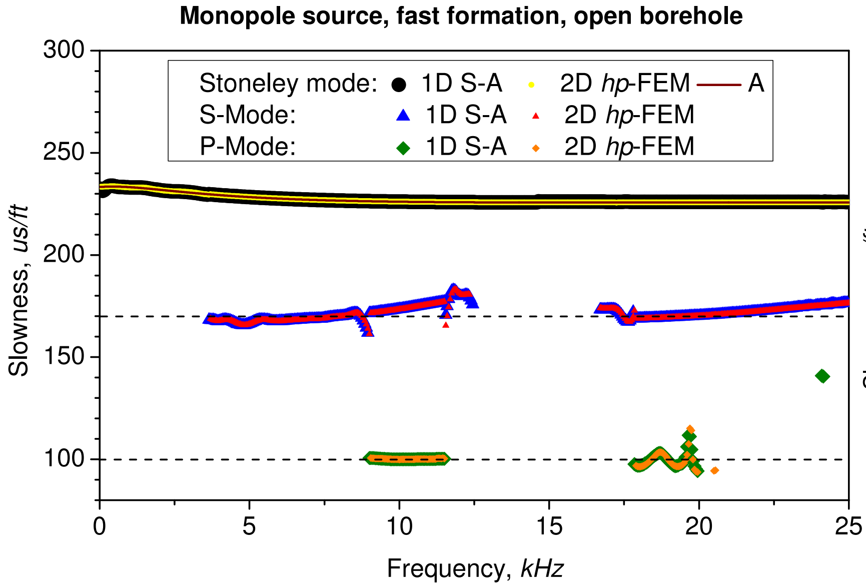

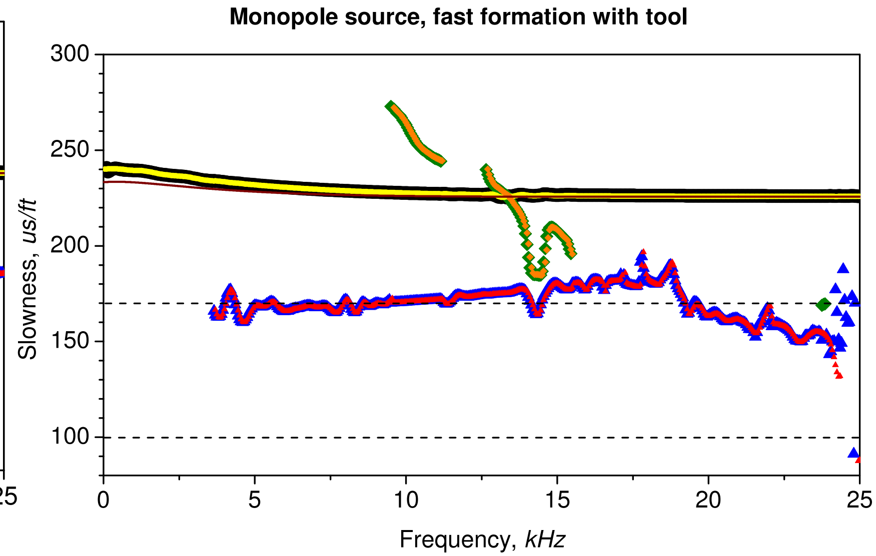

	P-wave		S-wave		Density
	V_p $[m/s]$	$1/V_p$ $[\mu s/ft]$	V_s $[m/s]$	$1/V_s$ $[\mu s/ft]$	ρ $[kg/m^3]$
fluid	1524	200.0	—	—	1100
fast form.	3048	100.0	1793	170.0	2200
tool	5860	52.0	3130	97.4	7800

sonic simulations

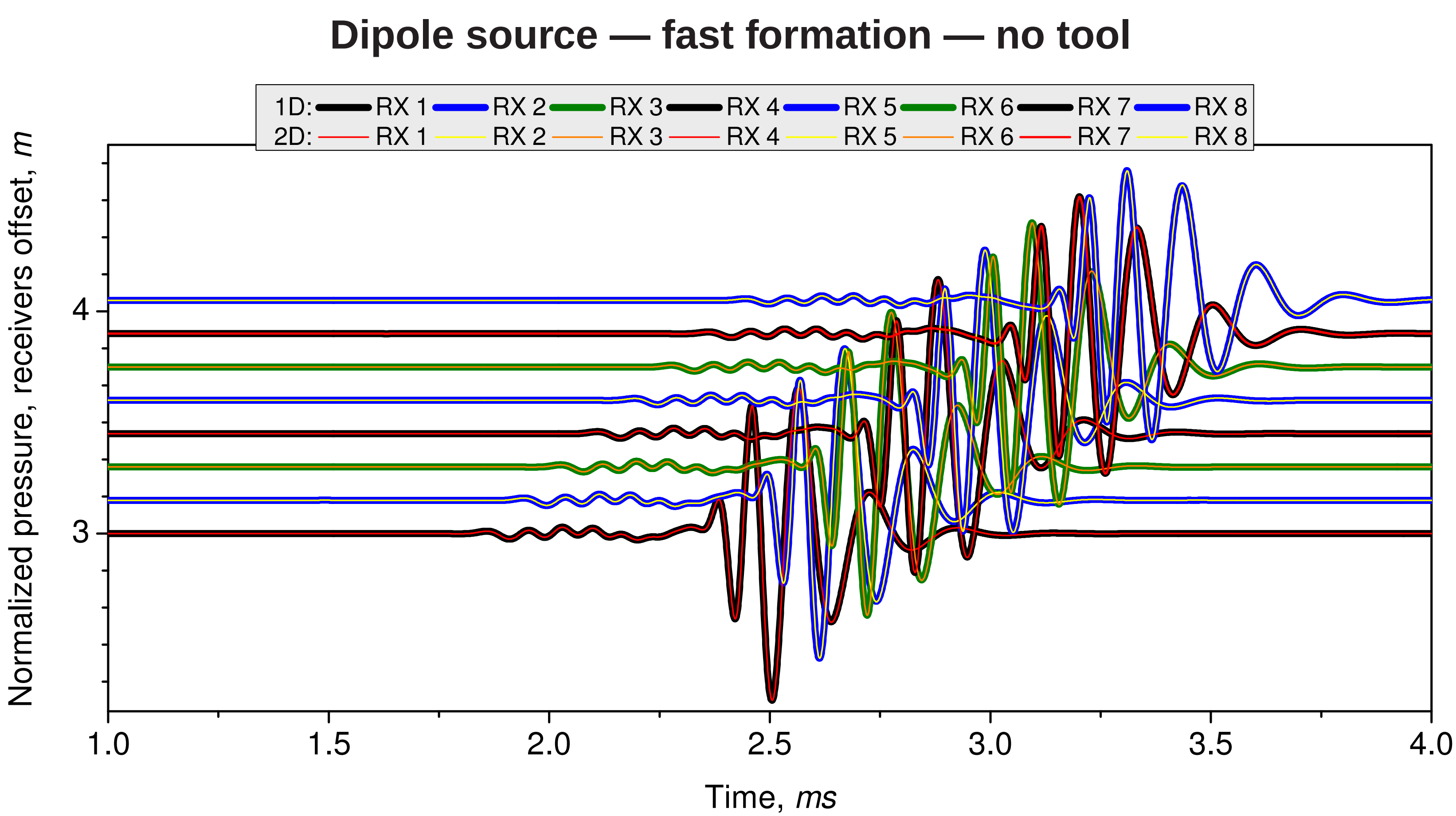

sonic simulations

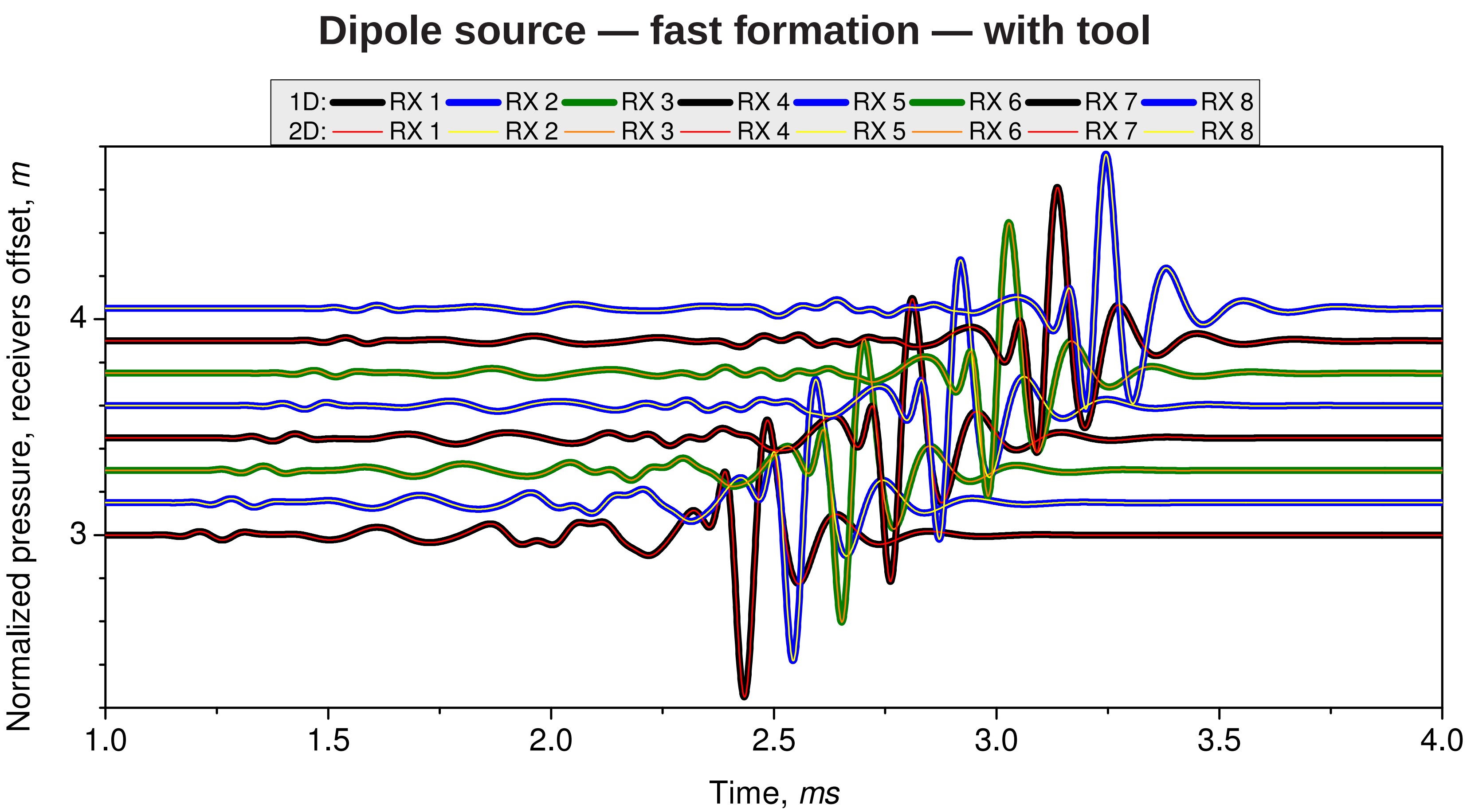

sonic simulations

Dipole source — fast formation

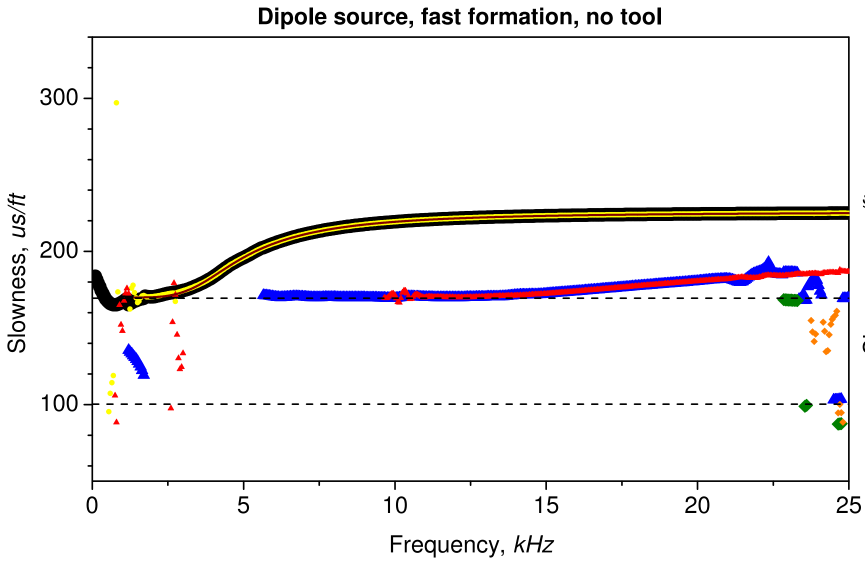

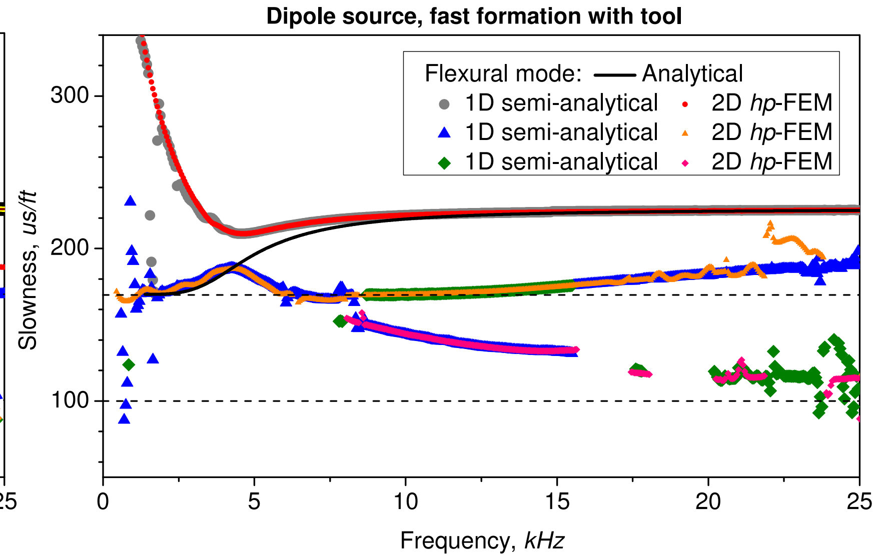

	P-wave		S-wave		Density
	$V_p\ [m/s]$	$1/V_p\ [\mu s/ft]$	$V_s\ [m/s]$	$1/V_s\ [\mu s/ft]$	$\rho\ [kg/m^3]$
fluid	1524	200.0	—	—	1100
fast form.	3048	100.0	1793	170.0	2200
tool	5860	52.0	3130	97.4	7800

sonic simulations

Direct calculation of dispersion curves

Dispersion curves contain the information about the slowness of the formation.

- dispersion curves are smooth with respect to variations in frequency,
- it is enough to calculate results only for a few frequencies (below 50)
- further reduction of the number of needed frequencies to 10 possible when only V_p (high frequencies) and V_s (low frequencies) are needed.

$\Rightarrow$ **Dispersion curves are obtained directly from frequency domain results.**

- no need to use in the simulations a Ricker wavelet (neither any other wavelet),
- the added stability of the problem,
- better performance of PML in frequency domain,
- smaller complexity of the problem.

sonic simulations

Direct calculation of dispersion curves

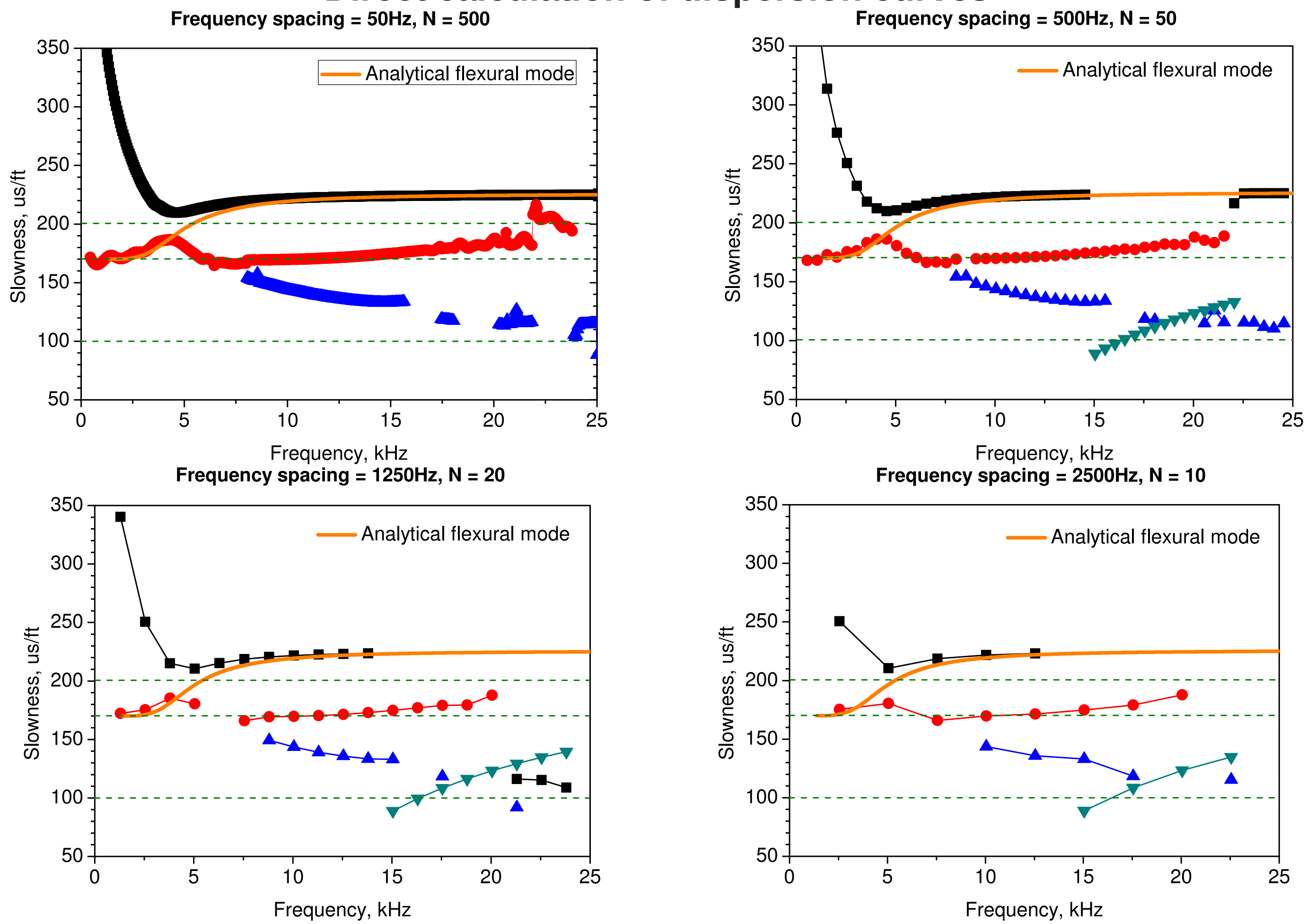

sonic simulations

Examples with layers

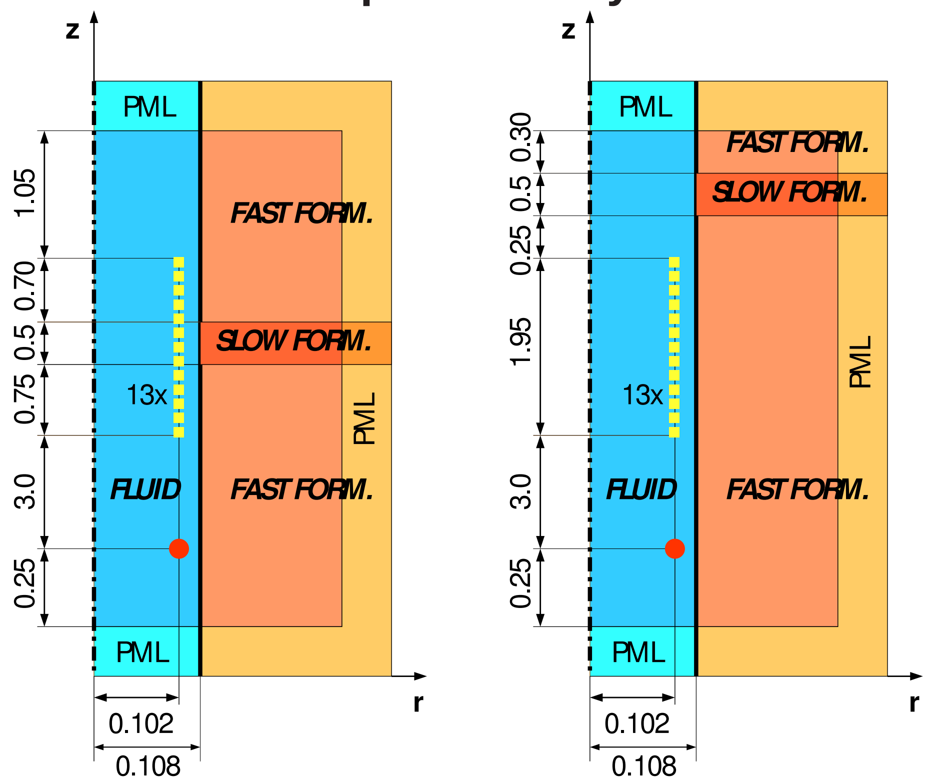

- **Formation thickness: 0.25m.**
- **Monopole/dipole source: Ricker wavelet, central frequency 8603 Hz.**

sonic simulations

Layers (1) — monopole (waveforms)

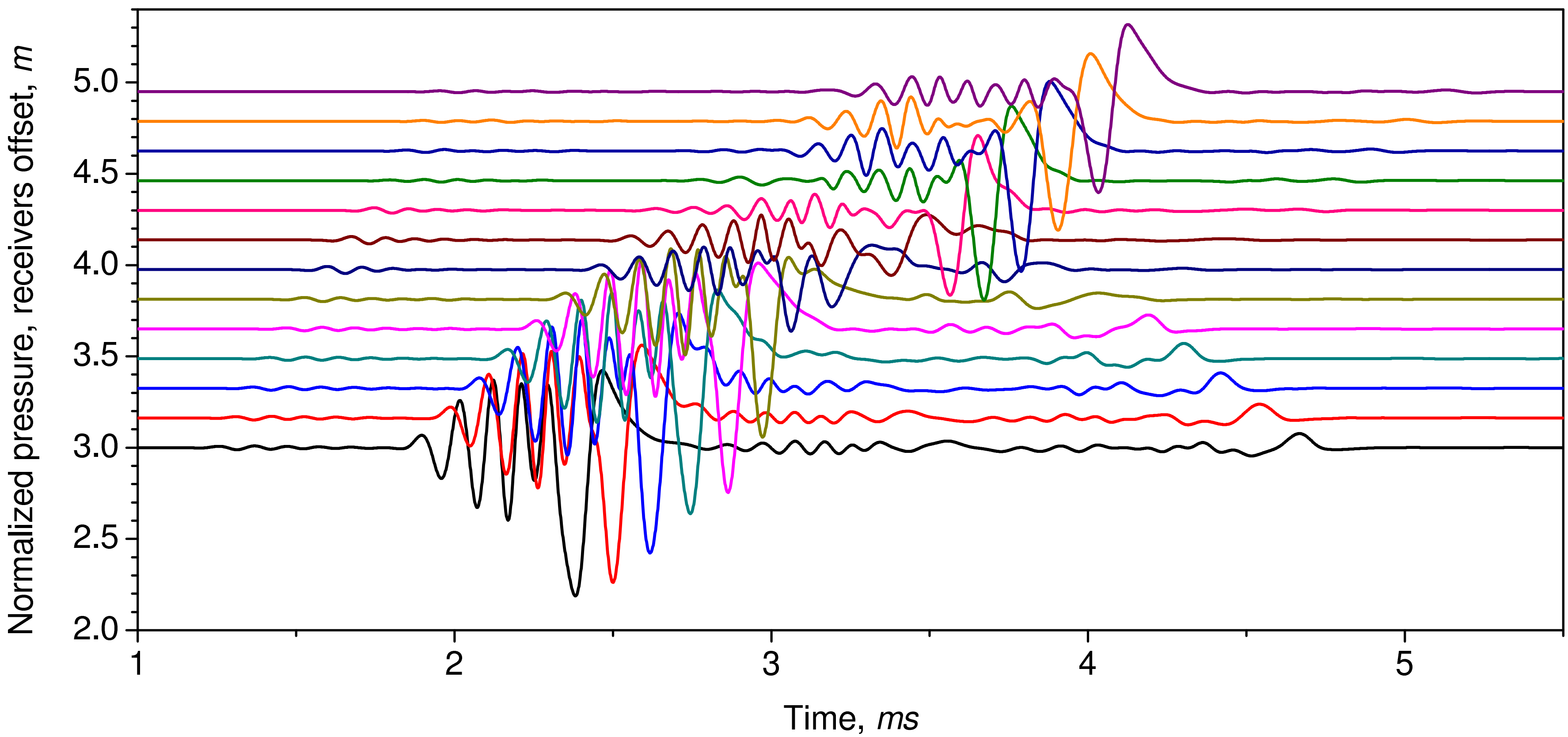

sonic simulations

Layers (2) — monopole (waveforms)

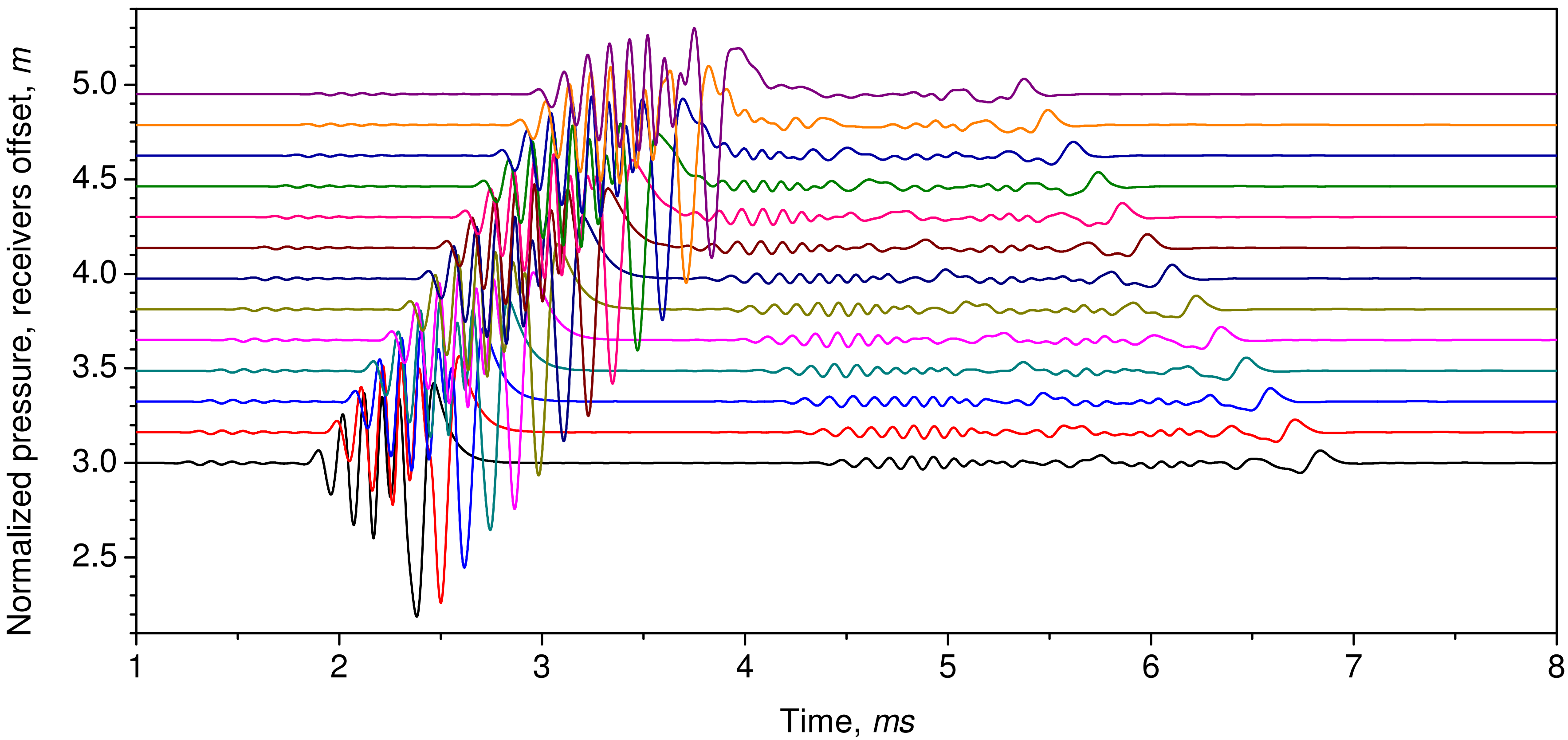

electromagnetic simulations

3D Variational Formulation

Time-Harmonic Maxwell's Equations

$\nabla \times \mathrm{H} = \mathring{\sigma}\mathrm{E} + \mathrm{J}^{imp}$	**Ampere's law ($\mathring{\sigma} = \sigma + j\omega\epsilon$)**
$\nabla \times \mathrm{E} = \mathring{\mu}\mathrm{H} + \mathrm{M}^{imp}$	**Faraday's law ($\mathring{\mu} = -j\omega\mu$)**
$\nabla \cdot (\epsilon \mathrm{E}) = \rho$	**Gauss' law of Electricity**
$\nabla \cdot (\mu \mathrm{H}) = 0$	**Gauss' law of Magnetism**

E-VARIATIONAL FORMULATION:

$$\begin{cases} \text{Find } \mathrm{E} \in \mathrm{E}_{\Gamma_E} + H_{\Gamma_E}(\mathrm{curl};\Omega) \text{ such that:} \\ \left\langle \nabla \times \mathrm{F}, \mathring{\mu}^{-1} \nabla \times \mathrm{E} \right\rangle_{L^2(\Omega)} - \left\langle \mathrm{F}, \mathring{\sigma}\mathrm{E} \right\rangle_{L^2(\Omega)} = \left\langle \mathrm{F}, \mathrm{J}^{imp} \right\rangle_{L^2(\Omega)} \\ -\left\langle \mathrm{F}_t, \mathrm{J}^{imp}_{\Gamma_H} \right\rangle_{L^2(\Gamma_H)} + \left\langle \nabla \times \mathrm{F}, \mathring{\mu}^{-1} \mathrm{M}^{imp} \right\rangle_{L^2(\Omega)} \quad \forall\, \mathrm{F} \in H_{\Gamma_E}(\mathrm{curl};\Omega) \end{cases}$$

electromagnetic simulations

Dimensionality Reduction for Maxwell's Equations

Solving a 3D problem is CPU time and memory intensive. In some cases, we may reduce the complexity of the problem by using Fourier analysis.

Borehole Problems

Cylindrical Coordinates

Fourier Series Expansion

$$\mathrm{E}(\phi) := \frac{1}{\sqrt{2\pi}} \sum_{n=-\infty}^{\infty} \mathcal{F}_n(\mathrm{E}) e^{jn\phi}$$

X-Well, CSEM Problems

Cartesian Coordinates

Fourier Transform

$$\mathrm{E}(x_1) := \frac{1}{\sqrt{2\pi}} \int_{\mathbb{R}} \mathcal{F}_r(\mathrm{E}) e^{jrx_1} dx_1$$

electromagnetic simulations

Fourier Series Expansion

Fourier series expansion **Inverse Fourier series expansion**

$$\mathcal{F}_n(\mathrm{E}) := \frac{1}{\sqrt{2\pi}} \int_0^{2\pi} \mathrm{E}(\phi) e^{-jn\phi} d\phi \quad ; \quad \mathrm{E}(\phi) = \frac{1}{\sqrt{2\pi}} \sum_{n=-\infty}^{\infty} \mathcal{F}_n(\mathrm{E}) e^{jn\phi}.$$

Main properties

- **Compatibility with differentiation** $\mathcal{F}_n(\frac{\partial \mathrm{E}}{\partial \phi}) = jn\mathcal{F}_n(\mathrm{E})$**:**

$$\mathcal{F}_n(\nabla \times \mathrm{E}) = \nabla^n \times (\mathcal{F}_n(\mathrm{E})),$$

where

$$\nabla^n \times \mathrm{E} := \left(\frac{jnE_z}{\rho} - \frac{\partial E_\phi}{\partial z}, \frac{\partial E_\rho}{\partial z} - \frac{\partial E_z}{\partial \rho}, \frac{1}{\rho}\frac{\partial(\rho E_\phi)}{\partial \rho} - \frac{jnE_\rho}{\rho} \right),$$

- L_2**-Orthogonality:**

$$\frac{1}{\sqrt{2\pi}} \int_0^{2\pi} e^{jn\phi} e^{-jm\phi} d\phi = \sqrt{2\pi}\delta_{nm} \ .$$

electromagnetic simulations

Fourier Transform

Fourier transform ; **Inverse Fourier transform**

$$\mathcal{F}_r(\mathrm{E}) := \frac{1}{\sqrt{2\pi}} \int_{\mathbb{R}} \mathrm{E}(x) e^{-jrx} dx \quad ; \quad \mathrm{E}(x) = \frac{1}{\sqrt{2\pi}} \int_{\mathbb{R}} \mathcal{F}_r(\mathrm{E}) e^{jrx} dr.$$

Main properties

- **Compatibility with differentiation** $\mathcal{F}_r(\frac{\partial \mathrm{E}}{\partial x}) = jr\mathcal{F}_r(\mathrm{E})$**:**

$$\mathcal{F}_r(\nabla \times \mathrm{E}) = \nabla^r \times (\mathcal{F}_r(\mathrm{E})),$$

where

$$\nabla^r \times \mathrm{E} := \left(\frac{\partial E_z}{\partial y} - \frac{\partial E_y}{\partial z}, \frac{\partial E_x}{\partial z} - jrE_z, jrE_y - \frac{\partial E_x}{\partial y} \right),$$

- L_2**-Orthogonality:**

$$\frac{1}{\sqrt{2\pi}} \int_{\mathbb{R}} e^{jrx} e^{-jsx} = \sqrt{2\pi} \delta_{sr} \ .$$

electromagnetic simulations

E-Variational Formulations (Cylindrical Coordinates)

FINITE ELEMENT —3D—:

$$\begin{cases} \text{Find } \mathrm{E} \in \mathrm{E}_{\Gamma_E} + H_{\Gamma_E}(\mathrm{curl};\Omega) \text{ such that:} \\ \langle \nabla \times \mathrm{F}, \mathring{\mu}^{-1} \nabla \times \mathrm{E} \rangle_{L^2(\Omega)} - \langle \mathrm{F}, \mathring{\sigma}\mathrm{E} \rangle_{L^2(\Omega)} = \langle \mathrm{F}, \mathrm{J}^{imp} \rangle_{L^2(\Omega)} \\ -\left\langle \mathrm{F}_t, \mathrm{J}^{imp}_{\Gamma_H} \right\rangle_{L^2(\Gamma_H)} + \langle \nabla \times \mathrm{F}, \mathring{\mu}^{-1} \mathrm{M}^{imp} \rangle_{L^2(\Omega)} \quad \forall\, \mathrm{F} \in H_{\Gamma_E}(\mathrm{curl};\Omega) \end{cases}$$

FOURIER FINITE ELEMENT —3D = Sequence of Coupled 2D Problems—:

$$\begin{cases} \text{Find } \mathrm{E} = \dfrac{1}{\sqrt{2\pi}} \displaystyle\sum_{n=-\infty}^{\infty} \mathcal{F}_n(\mathrm{E})\, e^{jn\phi}, \text{ where for each } n\text{:} \\ \mathcal{F}_n(\mathrm{E}) \in \mathcal{F}_n(\mathrm{E}_{\Gamma_{E,1D}}) + H_{\Gamma_{E,1D}}(\mathrm{curl}^n;\Omega_{2D}), \text{ and} \\ \displaystyle\sum_{m=-\infty}^{\infty} \langle \nabla^n \times \mathcal{F}_n(\mathrm{F}) \,,\, \mathcal{F}_{n-m}(\mathring{\mu}^{-1}) \nabla^m \times \mathcal{F}_m(\mathrm{E}) \rangle_{L^2(\Omega_{2D})} - \langle \mathcal{F}_n(\mathrm{F}) \,,\, \mathcal{F}_{n-m}(\mathring{\sigma}) \mathcal{F}_m(\mathrm{E}) \rangle_{L^2(\Omega_{2D})} \\ = \langle \mathcal{F}_n(\mathrm{F}) \,,\, \mathcal{F}_n(\mathrm{J}^{imp}) \rangle_{L^2(\Omega_{2D})} - \left\langle \mathcal{F}_n(\mathrm{F}_t) \,,\, \mathcal{F}_n(\mathrm{J}_S^{imp}) \right\rangle_{L^2(\Gamma_{H,1D})} \\ + \displaystyle\sum_{m=-\infty}^{\infty} \langle \nabla^n \times \mathcal{F}_n(\mathrm{F}) \,,\, \mathcal{F}_{n-m}(\mathring{\mu}^{-1}) \mathcal{F}_m(\mathrm{M}^{imp}) \rangle_{L^2(\Omega_{2D})} \quad \forall\, \mathcal{F}_n(\mathrm{F}) \in H_{\Gamma_{E,1D}}(\mathrm{curl}^n;\Omega_{2D}) \end{cases}$$

electromagnetic simulations

Cartesian system of coordinates: $\mathbf{x} = (x, y, z)$.
New non-orthogonal system of coordinates: $\zeta = (\zeta_1, \zeta_2, \zeta_3)$.

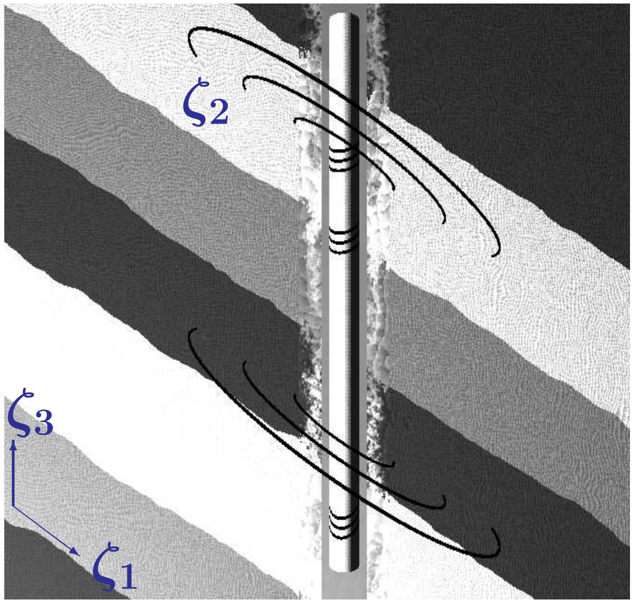

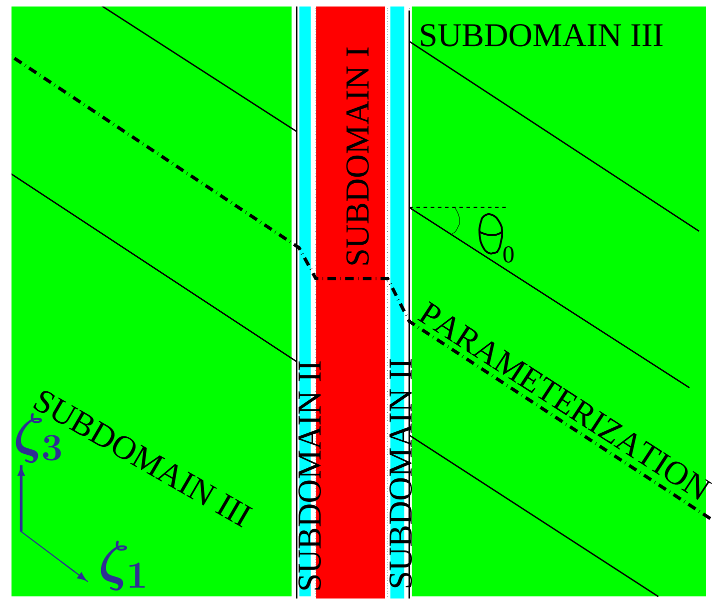

Subdomain I ; **Subdomain II** ; **Subdomain III**

$$\begin{cases} x = \zeta_1 \cos \zeta_2 \\ y = \zeta_1 \sin \zeta_2 \\ z = \zeta_3 \end{cases} ; \quad \begin{cases} x = \zeta_1 \cos \zeta_2 \\ y = \zeta_1 \sin \zeta_2 \\ z = \zeta_3 + \tan \theta_0 \dfrac{\zeta_1 - \rho_1}{\rho_2 - \rho_1} \rho_2 \end{cases} ; \quad \begin{cases} x = \zeta_1 \cos \zeta_2 \\ y = \zeta_1 \sin \zeta_2 \\ z = \zeta_3 + \tan \theta_0 \zeta_1 \end{cases}$$

electromagnetic simulations

E-Variational Formulation in the New System of Coordinates ζ

In the new system of coordinates, we obtain:

3D FOURIER FINITE ELEMENT FORMULATION

— Sequence of "Weakly" Coupled 2D Problems —

$$
\left\{
\begin{aligned}
&\text{Find } \mathrm{E} = \frac{1}{\sqrt{2\pi}} \sum_{n=-\infty}^{\infty} \mathcal{F}_n(\mathrm{E})\, e^{jn\zeta_2}, \text{ where for each } n: \\
&\mathcal{F}_n(\mathrm{E}) \in \mathcal{F}_n(\mathrm{E}_{\Gamma_{E,1D}}) + H_{\Gamma_{E,1D}}(\mathrm{curl}^n; \Omega_{2D}), \text{ and} \\
&\sum_{m=-2}^{2} \left\langle \nabla^n \times \mathcal{F}_n(\mathrm{F}) \,,\, \mathcal{F}_{n-m}(\mathring{\mu}_{mod}^{-1}) \nabla^m \times \mathcal{F}_m(\mathrm{E}) \right\rangle_{L^2(\Omega_{2D})} - \left\langle \mathcal{F}_n(\mathrm{F}) \,,\, \mathcal{F}_{n-m}(\mathring{\sigma}_{mod}) \mathcal{F}_m(\mathrm{E}) \right\rangle_{L^2(\Omega_{2D})} \\
&\quad = \left\langle \mathcal{F}_n(\mathrm{F}) \,,\, \mathcal{F}_n(\mathrm{J}^{imp}) \right\rangle_{L^2(\Omega_{2D})} - \left\langle \mathcal{F}_n(\mathrm{F}_t) \,,\, \mathcal{F}_n(\mathrm{J}_S^{imp}) \right\rangle_{L^2(\Gamma_{H,1D})} \\
&\quad + \sum_{m=-2}^{2} \left\langle \nabla^n \times \mathcal{F}_n(\mathrm{F}) \,,\, \mathcal{F}_{n-m}(\mathring{\mu}_{mod}^{-1}) \mathcal{F}_m(\mathrm{M}^{imp}) \right\rangle_{L^2(\Omega_{2D})} \quad \forall\, \mathcal{F}_n(\mathrm{F}) \in H_{\Gamma_{E,1D}}(\mathrm{curl}^n; \Omega_{2D})
\end{aligned}
\right.
$$

Five Fourier modes are sufficient to represent EXACTLY the new material coefficients resulting from incorporating the change of coordinates.

electromagnetic simulations

E-Variational Formulations (Cylindrical Coordinates)

Assumption: For $n \neq m$ we assume $\mathcal{F}_{n-m}(\mathring{\mu}^{-1}) = \mathcal{F}_{n-m}(\mathring{\sigma}^{-1}) = 0$.

FOURIER FINITE ELEMENT —2.5D = Sequence of Uncoupled 2D Problems—:

$$\begin{cases} \text{Find } \mathrm{E} = \dfrac{1}{\sqrt{2\pi}} \displaystyle\sum_{n=-\infty}^{\infty} \mathcal{F}_n(\mathrm{E})\, e^{jn\phi}, \text{ where for each } n\text{:} \\ \mathcal{F}_n(\mathrm{E}) \in \mathcal{F}_n(\mathrm{E}_{\Gamma_{E,1D}}) + H_{\Gamma_{E,1D}}(\mathrm{curl}^n;\Omega_{2D}), \text{ and} \\ \left\langle \nabla^n \times \mathcal{F}_n(\mathrm{F}) \,,\, \mathcal{F}_n(\mathring{\mu}^{-1}) \nabla^n \times \mathcal{F}_n(\mathrm{E}) \right\rangle_{L^2(\Omega_{2D})} - \left\langle \mathcal{F}_n(\mathrm{F}) \,,\, \mathcal{F}_n(\mathring{\sigma}) \mathcal{F}_n(\mathrm{E}) \right\rangle_{L^2(\Omega_{2D})} \\ \quad = \left\langle \mathcal{F}_n(\mathrm{F}) \,,\, \mathcal{F}_n(\mathrm{J}^{imp}) \right\rangle_{L^2(\Omega_{2D})} - \left\langle \mathcal{F}_n(\mathrm{F}_t) \,,\, \mathcal{F}_n(\mathrm{J}_S^{imp}) \right\rangle_{L^2(\Gamma_{H,1D})} \\ \quad + \left\langle \nabla^n \times \mathcal{F}_n(\mathrm{F}) \,,\, \mathcal{F}_n(\mathring{\mu}^{-1}) \mathcal{F}_n(\mathrm{M}^{imp}) \right\rangle_{L^2(\Omega_{2D})} \quad \forall\, \mathcal{F}_n(\mathrm{F}) \in H_{\Gamma_{E,1D}}(\mathrm{curl}^n;\Omega_{2D}) \end{cases}$$

electromagnetic simulations

2D Variational Formulation (Axi-symmetric Problems)

If we further assume that $\mathcal{F}_n(\mathrm{J}^{imp}) = \mathcal{F}_n(\mathrm{J}_S^{imp}) = \mathcal{F}_n(\mathrm{M}^{imp}) = 0 \quad \forall n \neq 0$, then we obtain one uncoupled 2D problem. Now, $\mathrm{E} = \mathcal{F}_0(\mathrm{E})$.

E_ϕ -Variational Formulation (Azimuthal)

$$\begin{cases} \text{Find } E_\phi \in E_{\phi,D} + \tilde{H}_D^1(\Omega) \text{ such that:} \\ \left\langle \nabla \times \mathrm{F}_\phi, \mathring{\mu}_{\rho,z}^{-1} \nabla \times \mathrm{E}_\phi \right\rangle_{L^2(\Omega_{2D})} - \langle \mathrm{F}_\phi, \mathring{\sigma}_\phi \mathrm{E}_\phi \rangle_{L^2(\Omega_{2D})} = \left\langle F_\phi, J_\phi^{imp} \right\rangle_{L^2(\Omega_{2D})} \\ \quad - \left\langle F_\phi, J_{\phi,\tilde{\Gamma}_H}^{imp} \right\rangle_{L^2(\tilde{\Gamma}_H)} + \left\langle F_\phi, \mathring{\mu}_{\rho,z}^{-1} \mathrm{M}_{\rho,z}^{imp} \right\rangle_{L^2(\Omega_{2D})} \qquad \forall\, F_\phi \in \tilde{H}_D^1(\Omega) \end{cases}$$

$\mathrm{E}_{\rho,z}$ -Variational Formulation (Meridian)

$$\begin{cases} \text{Find } \mathrm{E}_{\rho,z} = (E_\rho, E_z) \in \mathrm{E}_D + \tilde{H}_D(\mathrm{curl};\Omega) \text{ such that:} \\ \left\langle \nabla \times \mathrm{F}_{\rho,z}, \mathring{\mu}_\phi^{-1} \nabla \times \mathrm{E}_{\rho,z}) \right\rangle_{L^2(\Omega_{2D})} - \langle \mathrm{F}_{\rho,z}, \mathring{\sigma}_{\rho,z} \mathrm{E}_{\rho,z} \rangle_{L^2(\Omega_{2D})} = \\ \quad \left\langle \mathrm{F}_{\rho,z}, \mathrm{J}_{\rho,z}^{imp} \right\rangle_{L^2(\Omega_{2D})} - \left\langle (\mathrm{F}_{\rho,z})_t, \mathrm{J}_{\rho,z,\tilde{\Gamma}_H}^{imp} \right\rangle_{L^2(\tilde{\Gamma}_H)} \\ \quad + \left\langle \mathrm{F}_{\rho,z}, \mathring{\mu}_\phi^{-1} \mathrm{M}_\phi^{imp} \right\rangle_{L^2(\Omega_{2D})} \qquad \forall\, (F_\rho, F_z) \in \tilde{H}_D(\mathrm{curl};\Omega) \end{cases}$$

electromagnetic simulations

2D Finite Elements + 1D Fourier

3D Problem (using a Fourier Finite Element Method):

- $H(\mathrm{curl})$ **(Nedelec elements) for the meridian components ($\mathrm{E}_{\rho,z}$), and**
- H^1 **(Lagrange elements) for the azimuthal component (E_ϕ).**

2.5D Problem (using a Fourier Finite Element Method):

- $H(\mathrm{curl})$ **(Nedelec elements) for the meridian components ($\mathrm{E}_{\rho,z}$), and**
- H^1 **(Lagrange elements) for the azimuthal component (E_ϕ).**

2D Problem:

- $H(\mathrm{curl})$ **(Nedelec elements) in terms of the meridian components ($\mathrm{E}_{\rho,z}$), or**
- H^1 **(Lagrange elements) in terms of the azimuthal component (E_ϕ).**

electromagnetic simulations

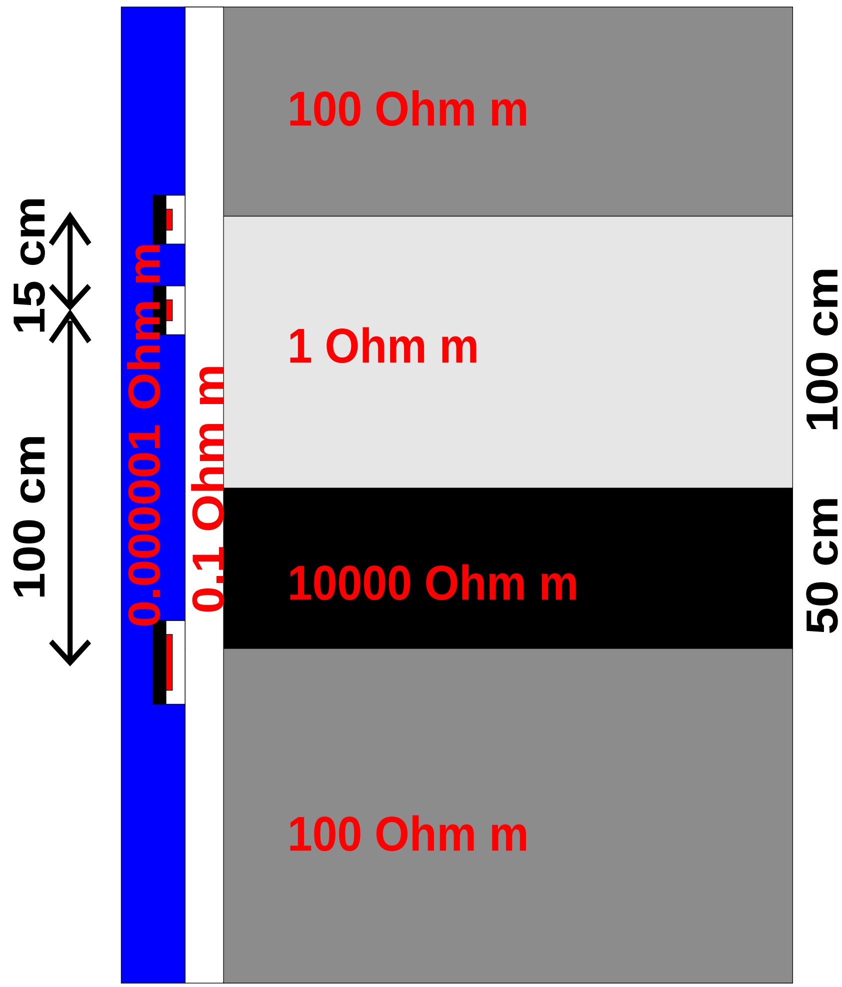

Description of Antennas

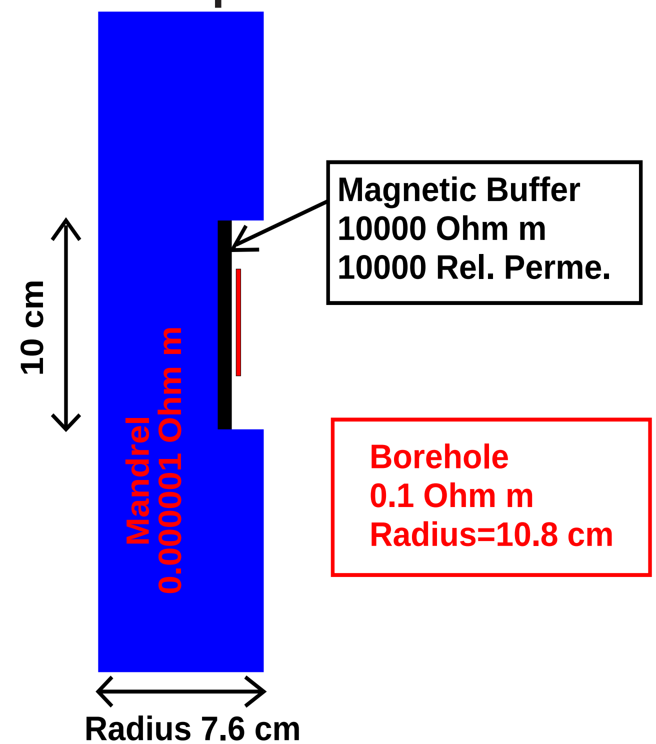

Goal: To Study the Effect of Invasion, Anistotropy, and Magnetic Permeability.

electromagnetic simulations

First. Vert. Diff. E_ϕ (solenoid). Position: 0.475m.

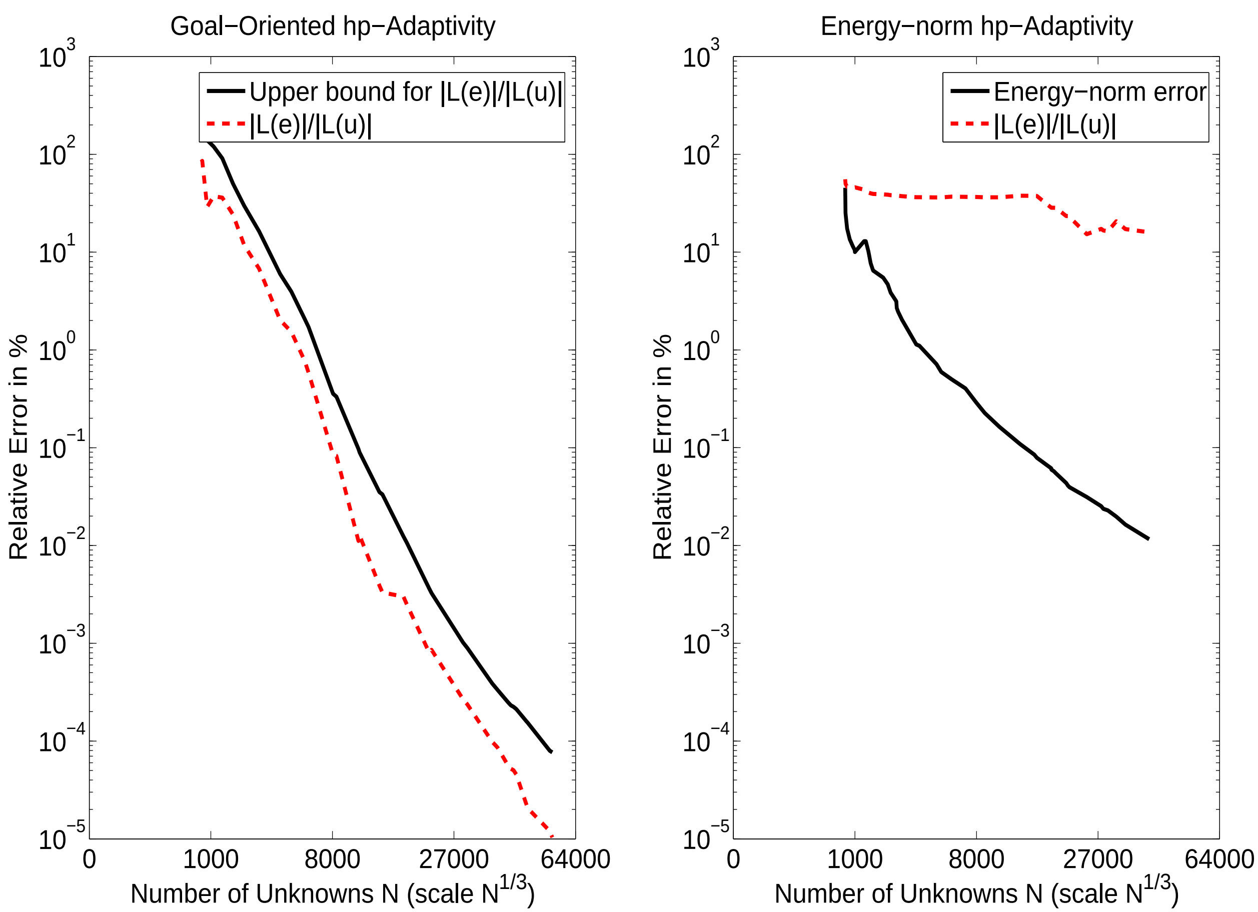

electromagnetic simulations

Goal-Oriented vs. Energy-norm hp-Adaptivity

Problem with Mandrel at 2 Mhz.

Continuous Elements (Goal-Oriented Adaptivity)

Quantity of Interest	Real Part	Imag Part
COARSE GRID	-0.1629862203E-01	-0.4016944732E-02
FINE GRID	-0.1629862347E-01	-0.4016944223E-02

Continuous Elements (Energy-Norm Adaptivity)

Quantity of Interest	Real Part	Imag Part
0.01% ENERGY ERROR	-0.1382759158E-01	-0.2989492851E-02

It is critical to use GOAL-ORIENTED adaptivity.

electromagnetic simulations

First. Vert. Diff. E_ϕ (solenoid). Position: 0.475m

ENERGY NORM HP-ADAPTIVITY

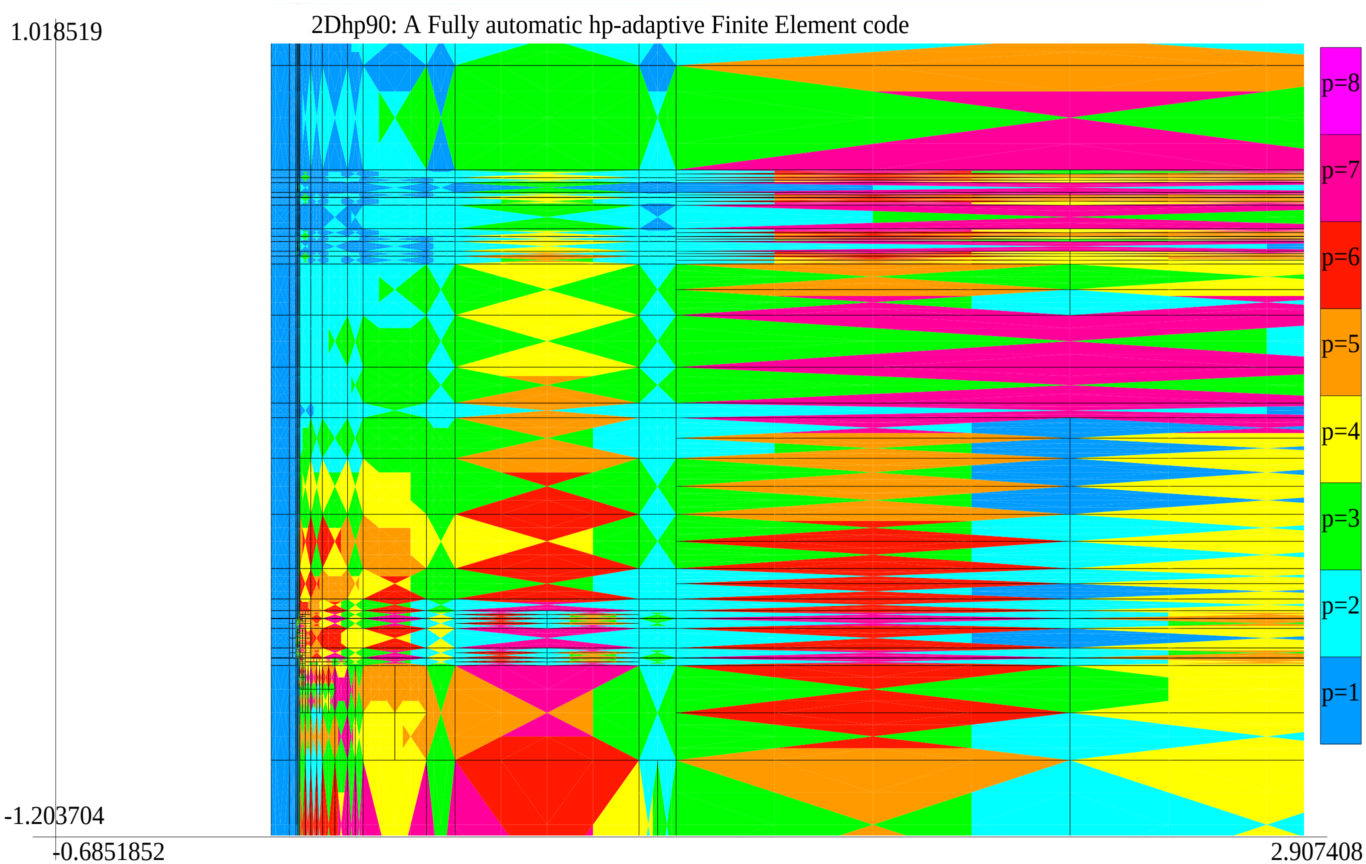

electromagnetic simulations

First. Vert. Diff. E_ϕ (solenoid). Position: 0.475m

GOAL-ORIENTED HP-ADAPTIVITY

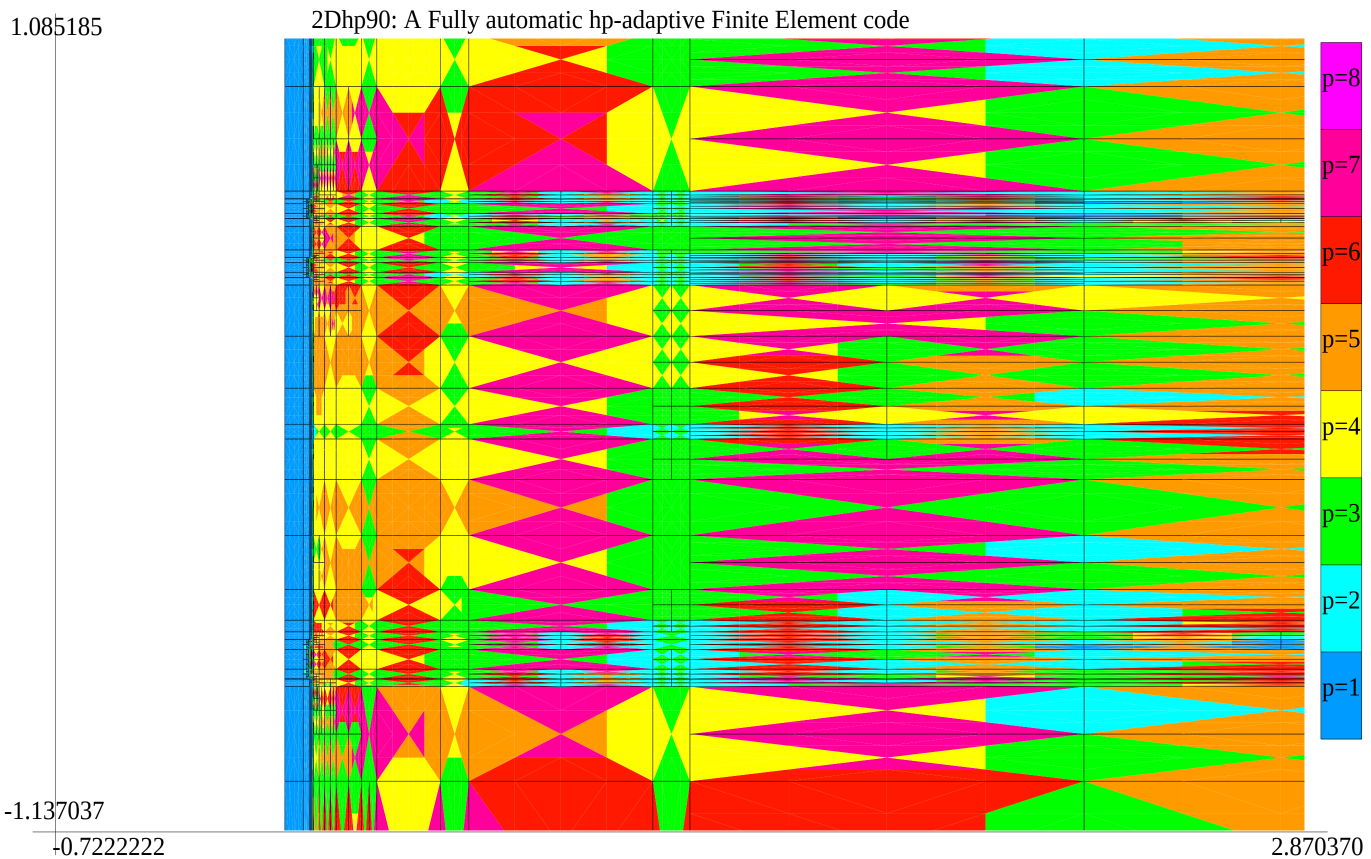

electromagnetic simulations

First. Vert. Diff. E_ϕ (solenoid). Position: 0.475m

GOAL-ORIENTED HP-ADAPTIVITY (ZOOM)

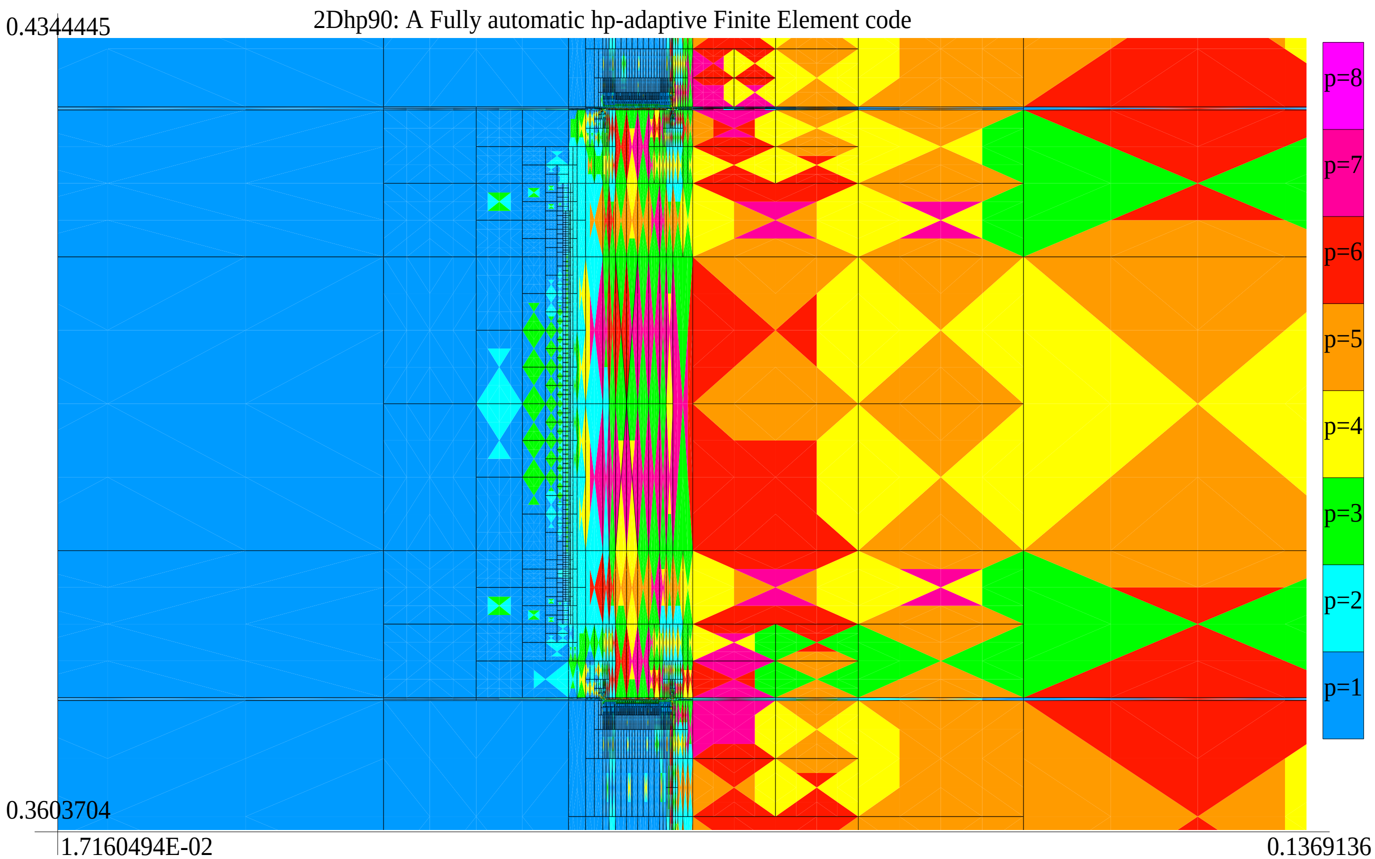

electromagnetic simulations

Simulation of Through Casing Resistivity Measurements

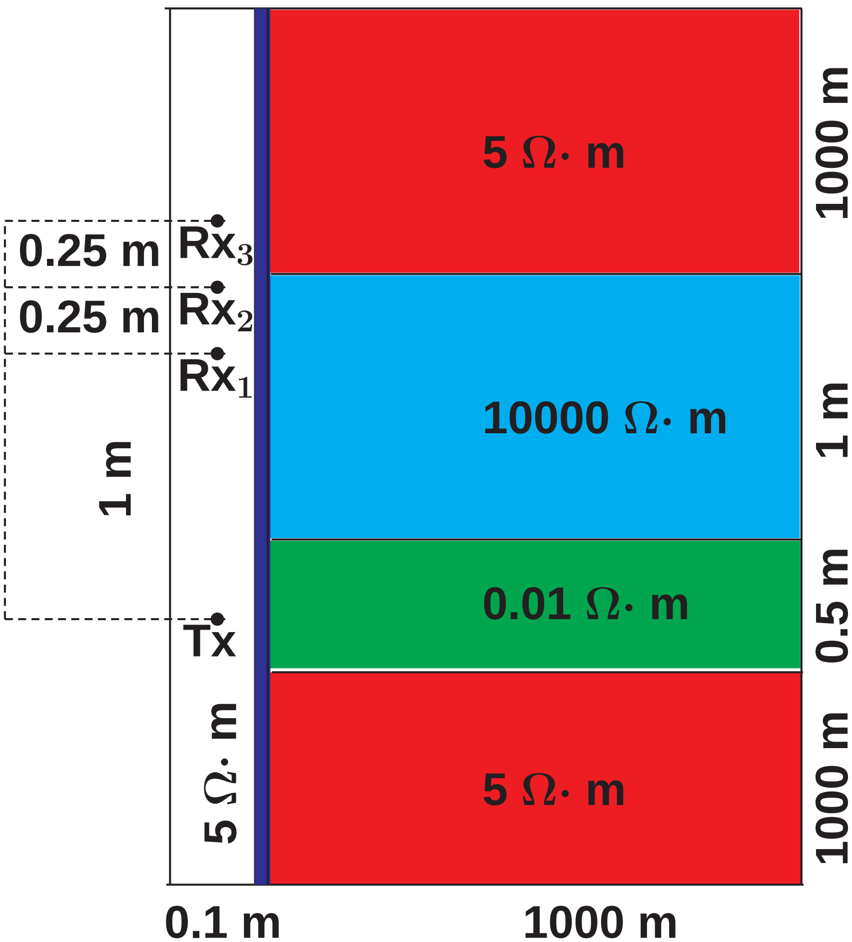

Left Figure:
- Axial-symmetric model
- One current electrode (emitter)
- Three voltage electrodes (collectors)

Objective:
- Compute second diff. of potential for various depth angles and possibly with water invasion

Method of solution:
- Fourier series expansion + change of coordinates + 2D goal-oriented hp-FEM

electromagnetic simulations

Through Casing Resistivity Measurements (Casing Conductivity)

Casing Resistivity=$10^{-5}\Omega\cdot$ m

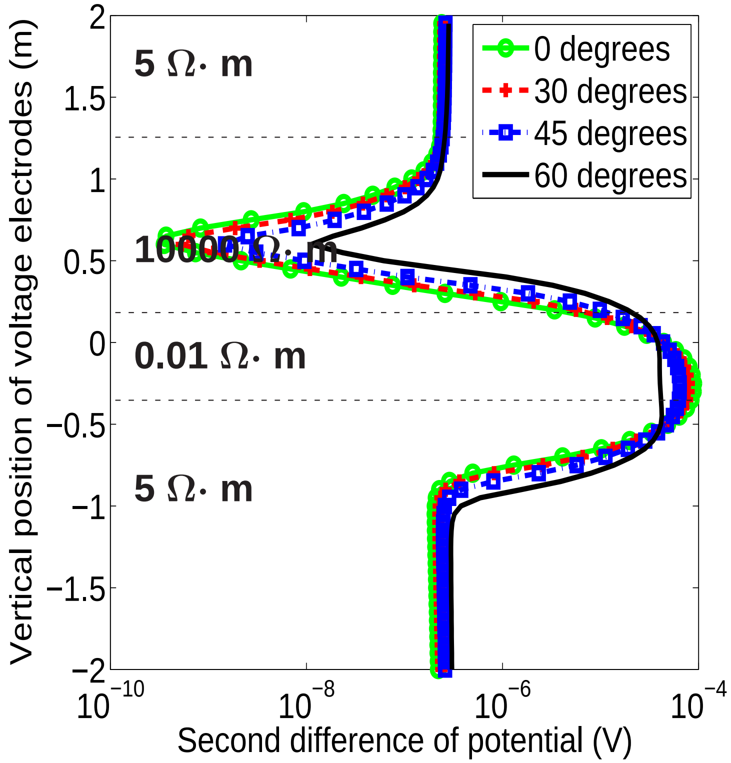

Casing Resistivity=$2.3\times10^{-7}\Omega\cdot$ m

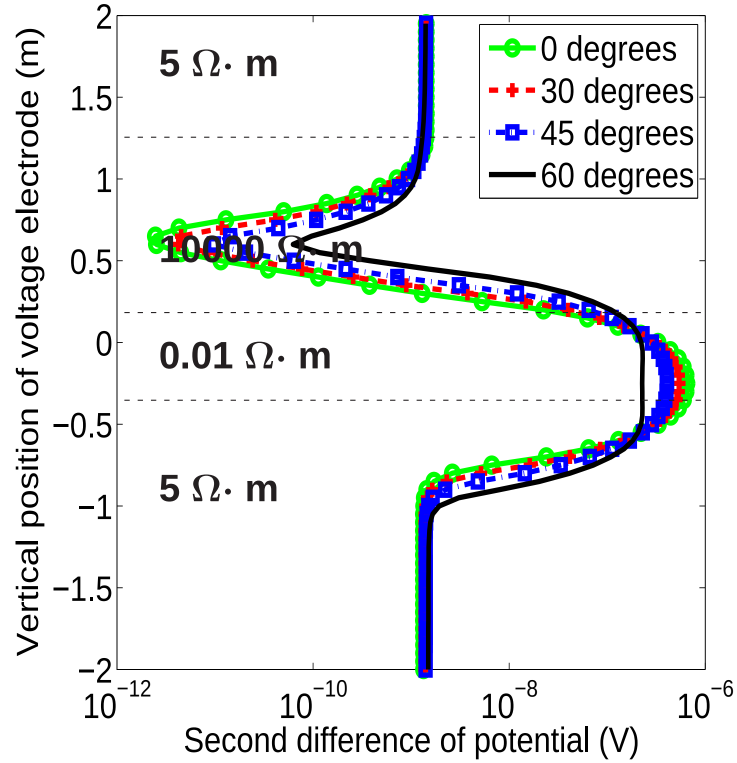

Qualitatively, results for various casing conductivities are similar even for deviated wells.

electromagnetic simulations

Through Casing Resistivity Measurements (Invasion)

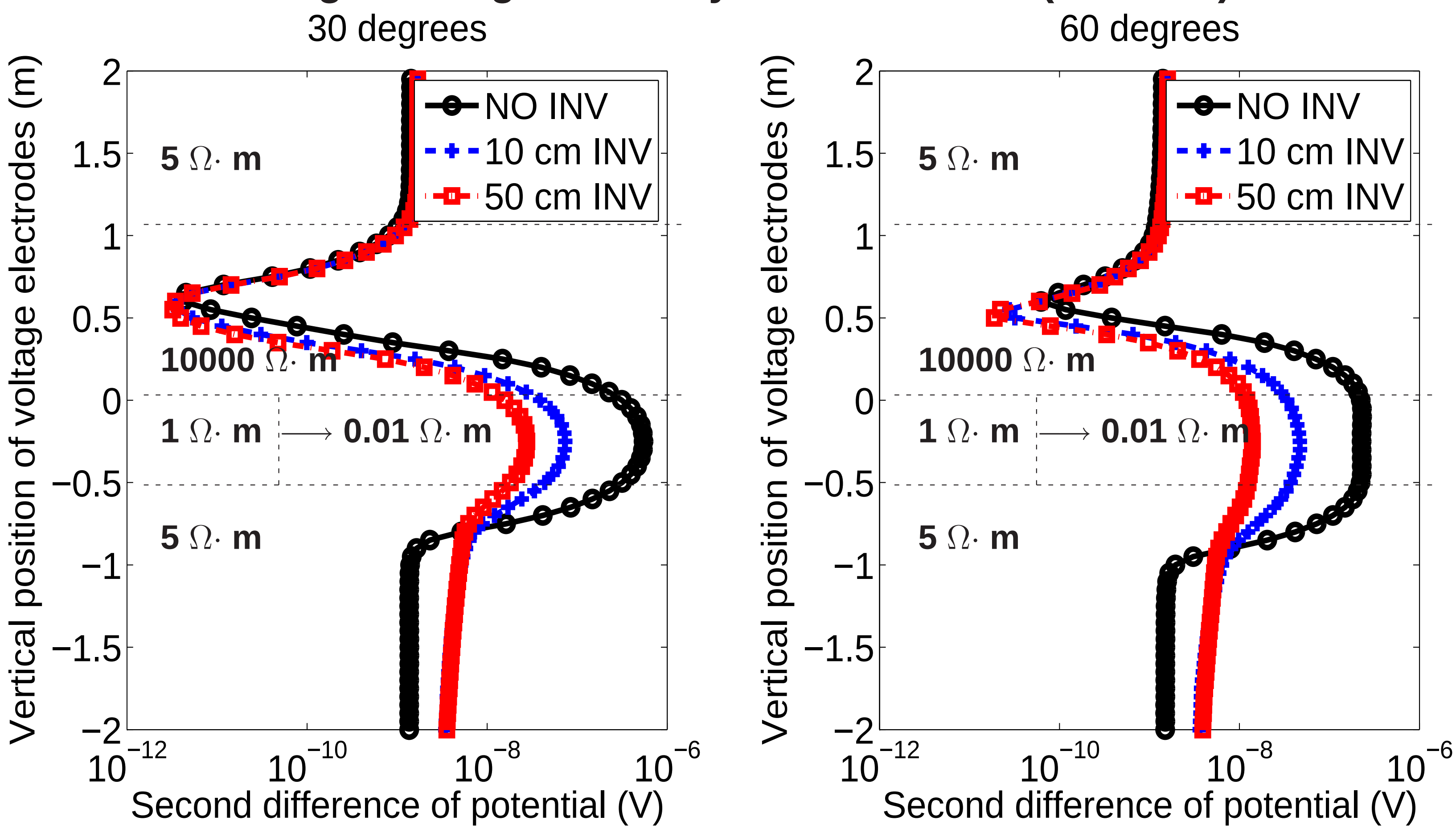

electromagnetic simulations

Through Casing Resistivity Measurements (Invasion)

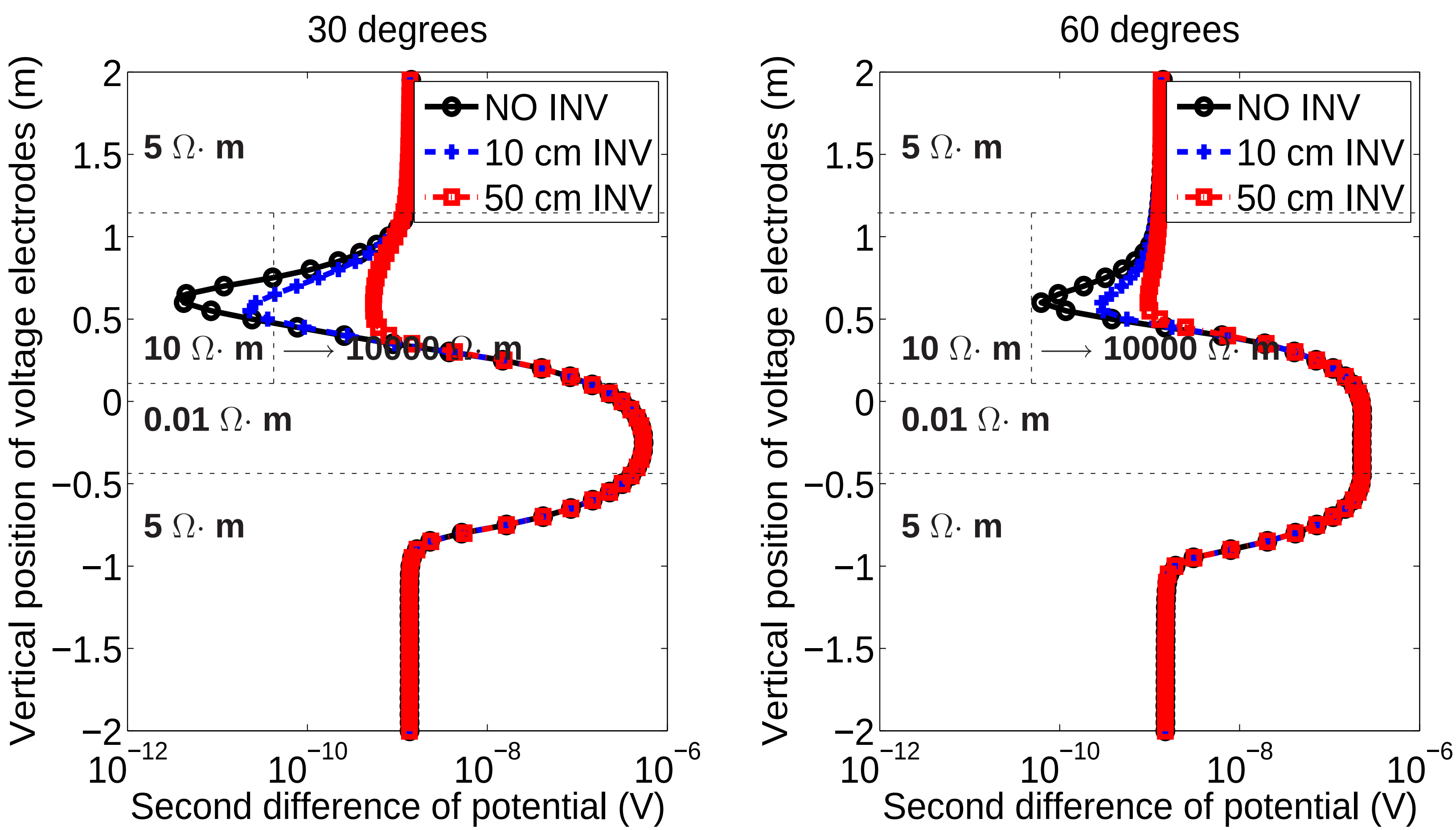

electromagnetic simulations

Model Problem and Verification

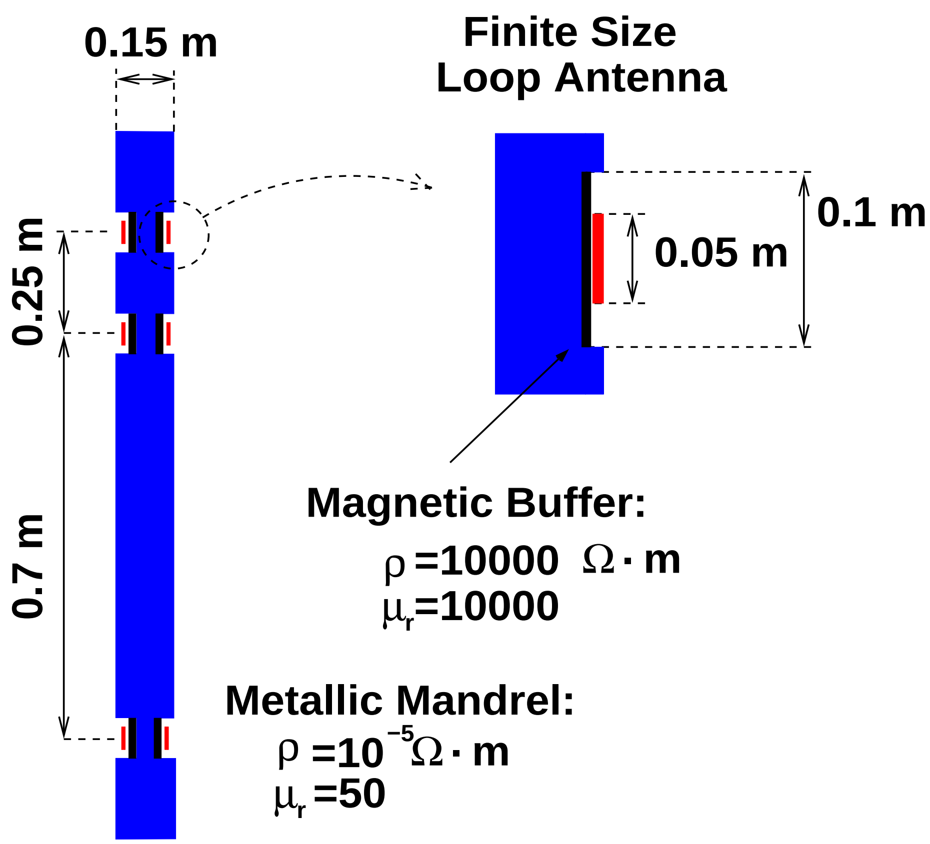

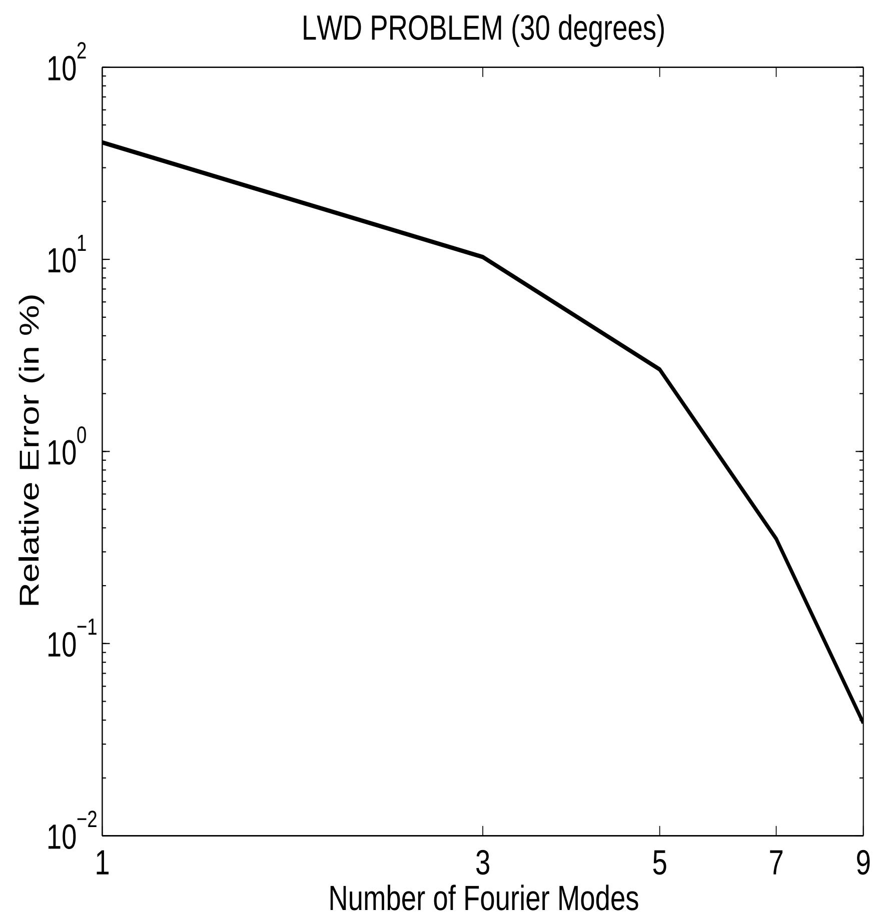

electromagnetic simulations

Dip Angle

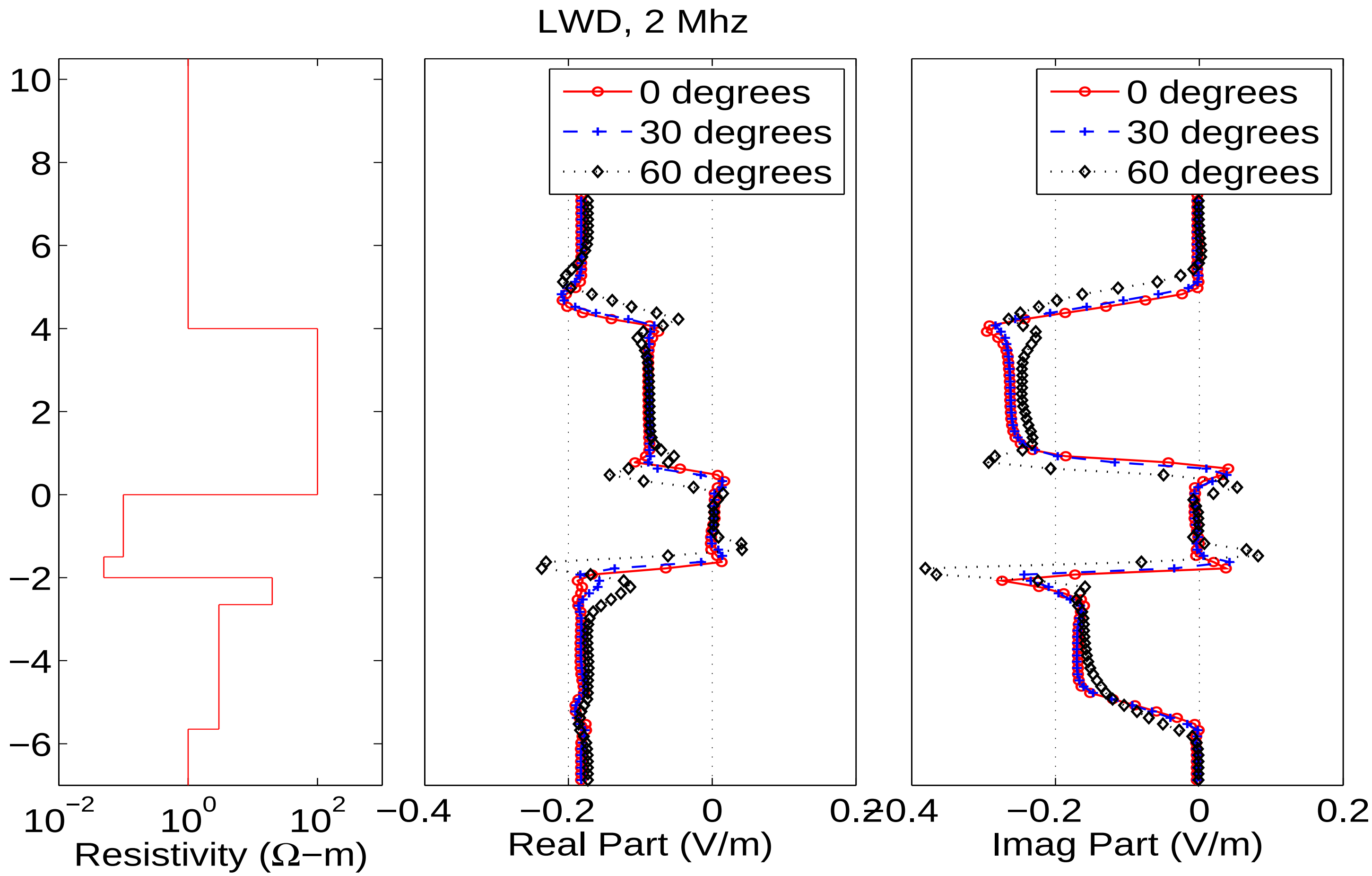

electromagnetic simulations

Dip Angle + Invasion

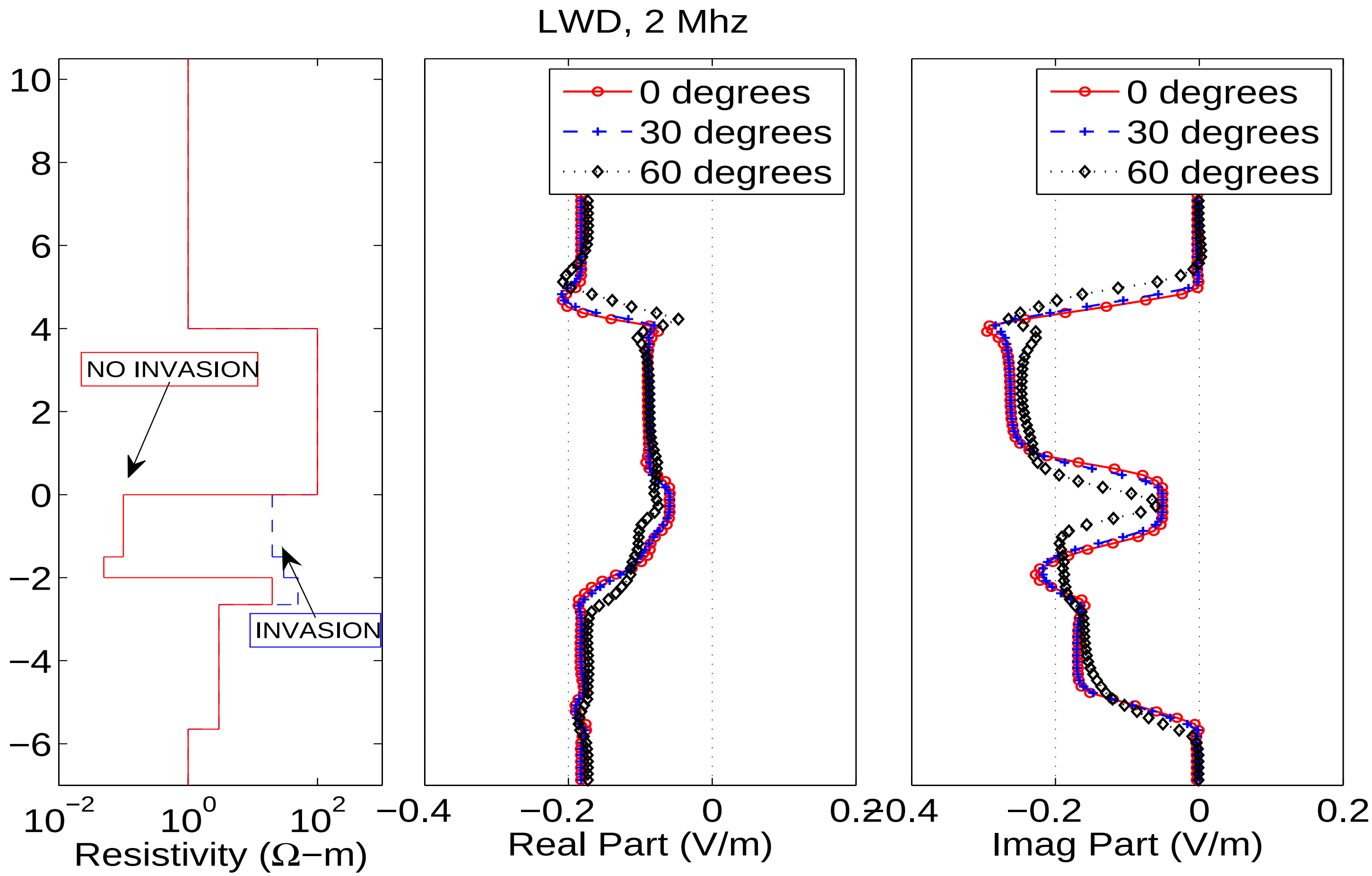

electromagnetic simulations

Dip Angle + Anisotropy

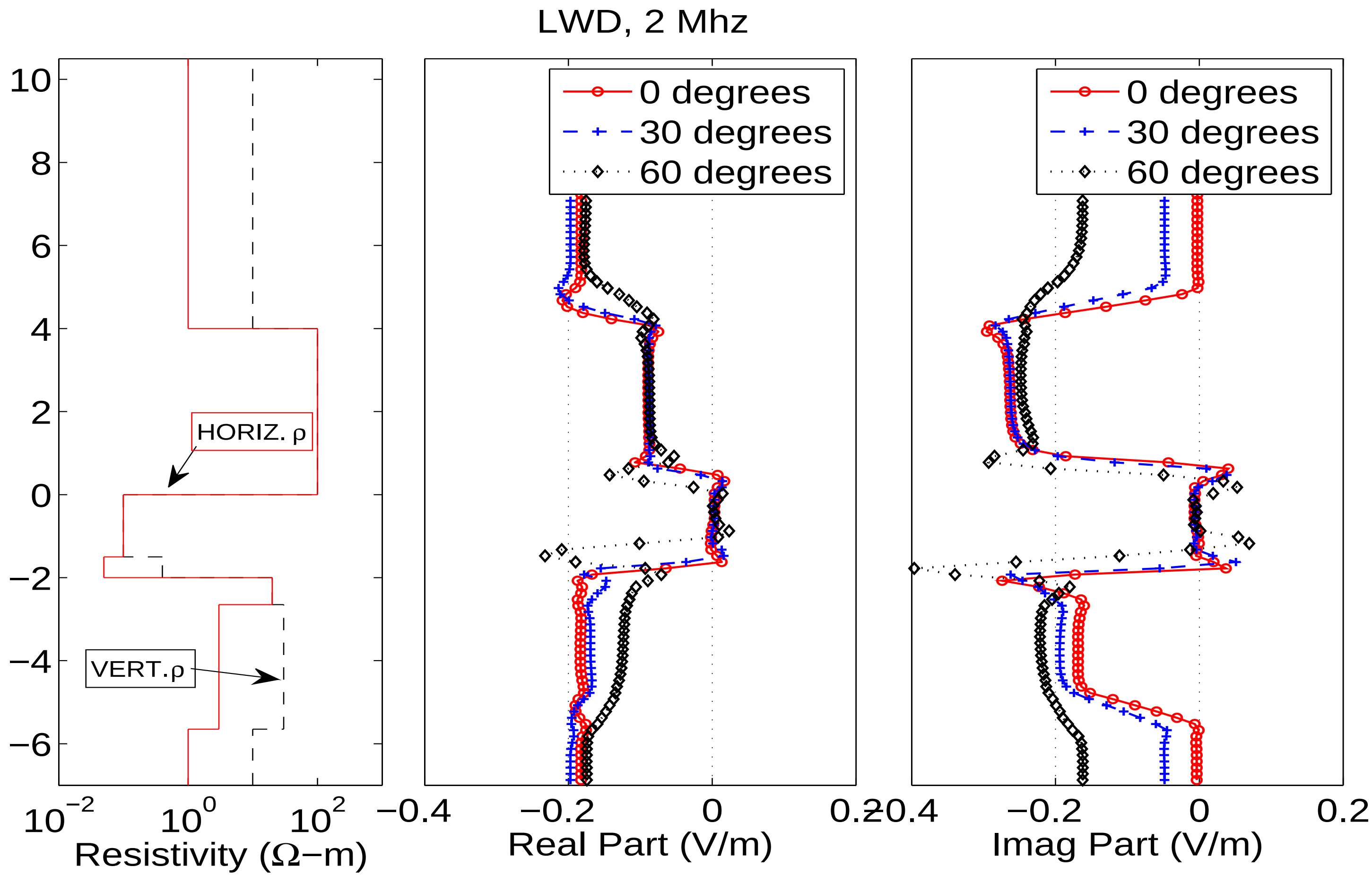

electromagnetic simulations

Dip Angle + Invasion + Anisotropy

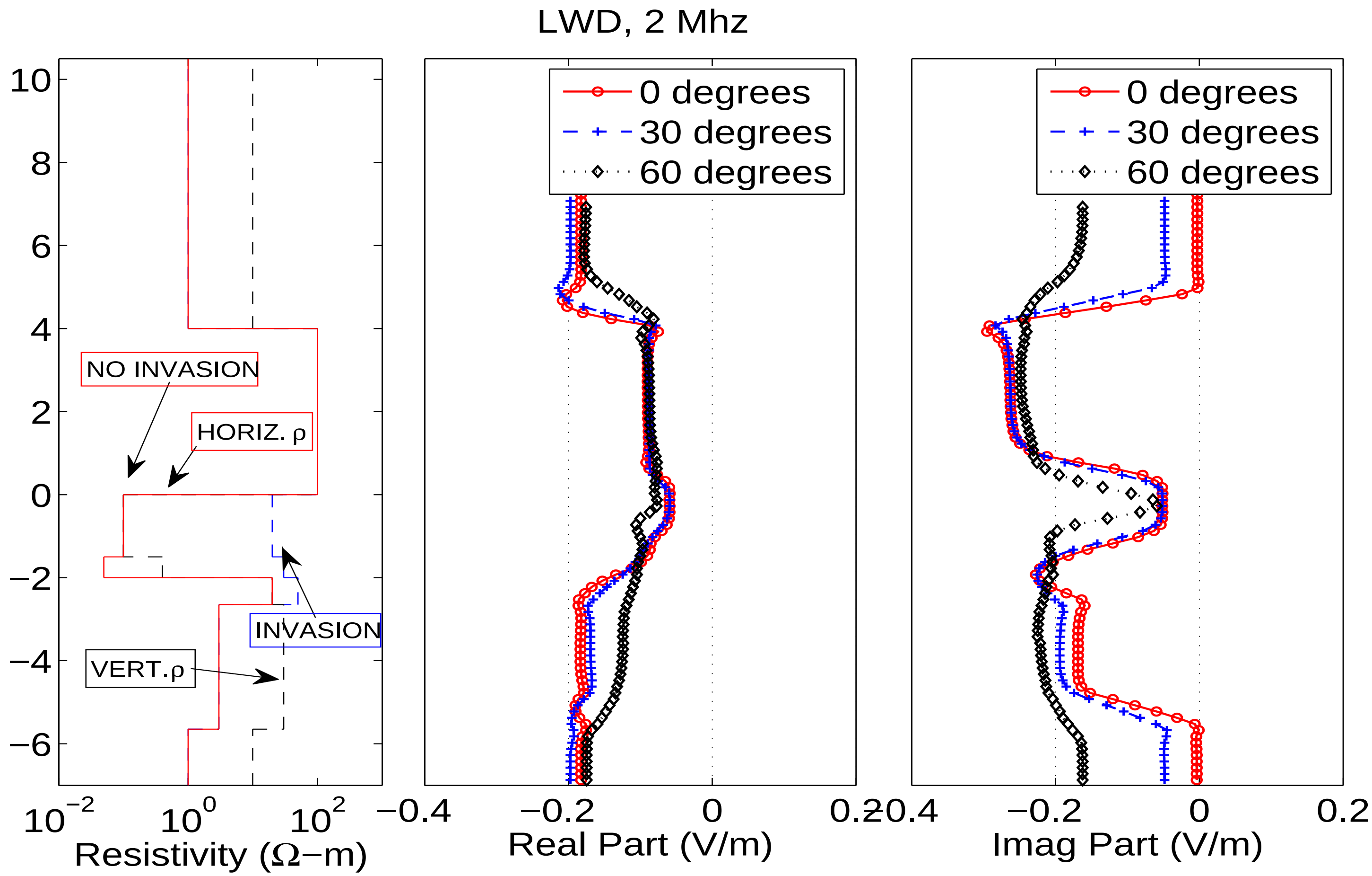

electromagnetic simulations

60-Degree Deviated Well

LWD, 2 Mhz

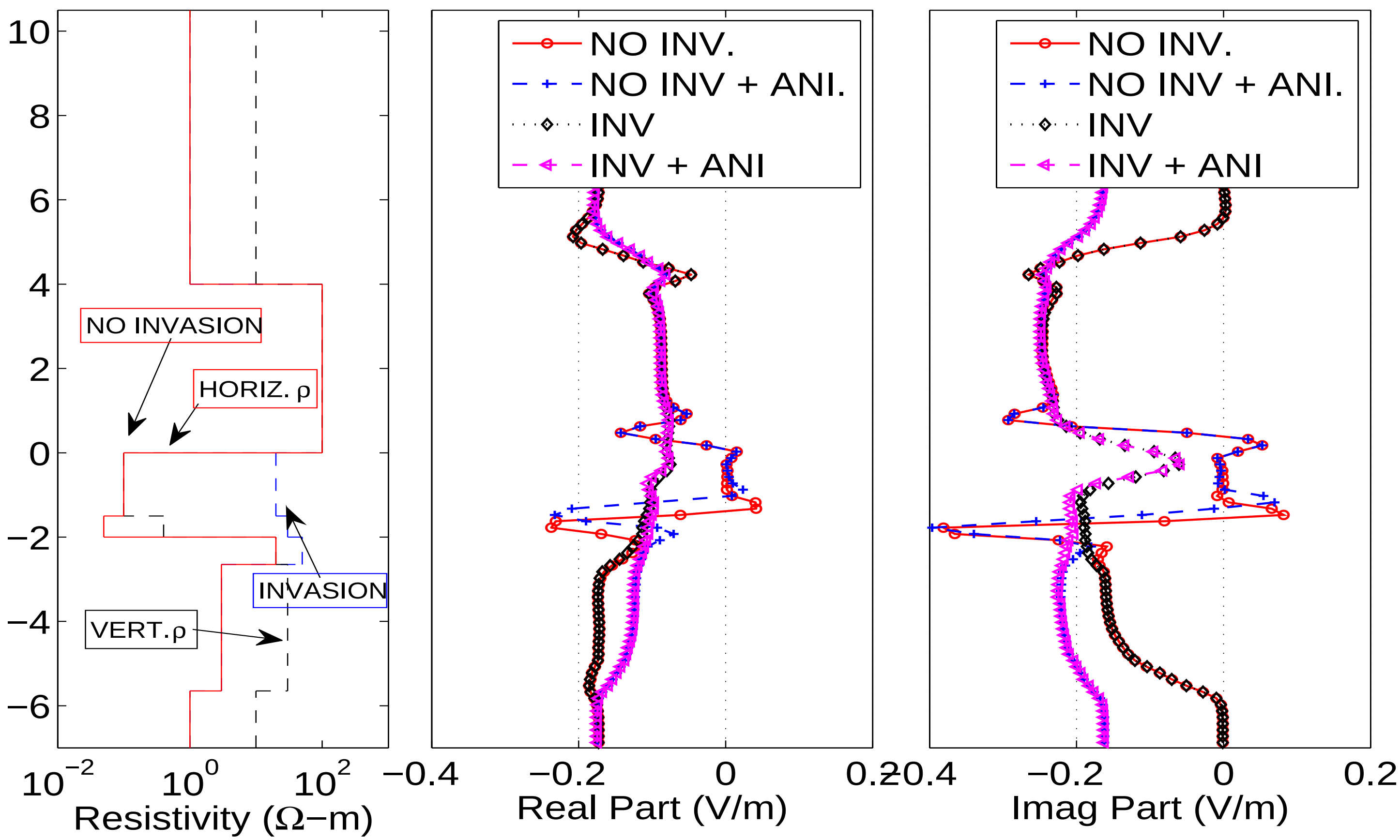

inversion problems

Variational Formulation (DC)

Notation:

$$B(u, v; \sigma) = < \nabla v, \sigma \nabla u >_{L^2(\Omega)} \qquad \textbf{(bilinear } u, v\textbf{)}$$

$$F_i(v) = < v, f_i >_{L^2(\Omega)} + < v, g_i >_{L^2(\partial\Omega)} \qquad \textbf{(linear } v\textbf{)}$$

$$L_i(u) = < l_i, u >_{L^2(\Omega)} + < h_i, u >_{L^2(\partial\Omega)} \qquad \textbf{(linear } u\textbf{)}$$

Direct Problem (homogeneous Dirichlet BC's):

$$\begin{cases} \text{Find } \hat{u}_i \in \text{V such that :} \\ B(\hat{u}_i, v; \sigma) = F_i(v) \quad \forall v \in V \end{cases}$$

Dual (Adjoint) Problem:

$$\begin{cases} \text{Find } \hat{v}_i \in \text{V such that :} \\ B(u, \hat{v}_i; \sigma) = L_i(u) \quad \forall u \in V \end{cases}$$

inversion problems

Variational Formulation (AC)

Notation:

$$B(\mathrm{E},\mathrm{F};\sigma) =< \nabla\times\mathrm{F}, \mu^{-1}\nabla\times\mathrm{E} >_{L^2(\Omega)} - < \mathrm{F}, (\omega^2\epsilon - j\omega\sigma)\mathrm{E} >_{L^2(\Omega)}$$

$$F_i(\mathrm{F}) = -j\omega < \mathrm{F}, \mathrm{J}_i^{imp} >_{L^2(\Omega)} + j\omega < \mathrm{F}, \mathrm{J}_{S,i}^{imp} >_{L^2(\partial\Omega)}$$

$$L_i(\mathrm{E}) =< \mathrm{J}_i^{adj}, \mathrm{E} >_{L^2(\Omega)} + < \mathrm{J}_{S,i}^{adj}, \mathrm{E} >_{L^2(\partial\Omega)}$$

Direct Problem (homogeneous Dirichlet BC's):

$$\begin{cases} \text{Find } \hat{\mathrm{E}}_i \in \text{W such that :} \\ B(\hat{\mathrm{E}}_i, \mathrm{F}; \sigma) = F_i(\mathrm{F}) \quad \forall \mathrm{F} \in W \end{cases}$$

Dual (Adjoint) Problem:

$$\begin{cases} \text{Find } \hat{\mathrm{F}}_i \in \text{W such that :} \\ B(\mathrm{E}, \hat{\mathrm{F}}_i; \sigma) = L_i(\mathrm{E}) \quad \forall \mathrm{E} \in W \end{cases}$$

inversion problems

Constrained Nonlinear Optimization Problem

Cost Functional:

$$\begin{cases} \text{Find } \boldsymbol{\sigma} > 0 \text{ such that it minimizes } C_\beta(\boldsymbol{\sigma})\text{, where :} \\ C_\beta(\boldsymbol{\sigma}) = ||W_m(L(\hat{u}_{\boldsymbol{\sigma}}) - M)||^2_{l_2} + \beta||R(\boldsymbol{\sigma} - \boldsymbol{\sigma}_0)||^2_{L_2} \, , \end{cases}$$

where

M_i denotes the i-th measurement, $M = (M_1, ..., M_n)$

L_i is the i-th quantity of interest, $L = (L_1, ..., L_n)$

$$||M||^2_{l_2} = \sum_{i=1}^{n} M_i^2 \quad ; \quad ||R(\boldsymbol{\sigma} - \boldsymbol{\sigma}_0)||^2_{L_2} = \int (R(\boldsymbol{\sigma} - \boldsymbol{\sigma}_0))^2$$

β is the relaxation parameter, σ_0 is given, W_m are weights

Main objective (inversion problem): Find $\hat{\boldsymbol{\sigma}} = \min\limits_{\boldsymbol{\sigma} > 0} C_\beta(\boldsymbol{\sigma})$

inversion problems

Solving a Constrained Nonlinear Optimization Problem

We select the following deterministic iterative method:

$$\boldsymbol{\sigma}^{(n+1)} = \boldsymbol{\sigma}^{(n)} + \boldsymbol{\alpha}^{(n)} \boldsymbol{\delta\sigma}^{(n)}$$

- **How to find a search direction $\boldsymbol{\delta\sigma}^{(n)}$?**
  - **We will employ a change of coordinates and a truncated Taylor's series expansion.**
- **How to determine the step size $\boldsymbol{\alpha}^{(n)}$?**
  - **Either with a fixed size or using an approximation for computing $\boldsymbol{L}(\boldsymbol{\sigma}^{(n)} + \boldsymbol{\alpha}^{(n)}\boldsymbol{\delta\sigma}^{(n)})$.**
- **How to guarantee that the nonlinear constraints will be satisfied?**
  - **Imposing the Karush-Kuhn-Tucker (KKT) conditions or with a penalization method, or via a change of variables.**

inversion problems

Search Direction Method

Change of coordinates:

$$h(s) = \sigma \quad => \text{ Find } \hat{s} = \min_{h(s)>0} C_\beta(s)$$

Taylor's series expansion:

A) $C_\beta(s+\delta s) \approx C_\beta(s) + \delta s \nabla C_\beta(s) + 0.5 \delta s^2 H_{C_\beta}(s)$

B) $L(s+\delta s) \approx L(s) + \delta s \nabla L(s)\ ,\ R(s+\delta s) = R(s) + \delta s \nabla R(s)$

Expansion A) leads to the Newton-Raphson method.

Expansion B) leads to the Gauss-Newton method.

Expansion A) with $H_{C_\beta} = I$ leads to the steepest descent method.

Higher-order expansions require from higher-order derivatives.

inversion problems

Computation of Jacobian Matrix

Using the Fréchet Derivative:

$$\frac{\partial L_i(\hat{u}_i)}{\partial s_j} = B\left(\frac{\partial \hat{u}_i}{\partial s_j}, \hat{v}_i, h(s)\right) + B\left(\hat{u}_i, \frac{\partial \hat{v}_i}{\partial s_j}, h(s)\right) + B\left(\hat{u}_i, \hat{v}_i, \frac{\partial h(s)}{\partial s_j}\right)$$

$$\|$$

$$L_i\left(\frac{\partial \hat{u}_i}{\partial s_j}\right) = B\left(\frac{\partial \hat{u}_i}{\partial s_j}, \hat{v}_i, h(s)\right)$$

$$\|$$

$$F_i\left(\frac{\partial \hat{v}_i}{\partial s_j}\right) = B\left(\hat{u}_i, \frac{\partial \hat{v}_i}{\partial s_j}, h(s)\right)$$

Therefore, we conclude:

$$\text{Jacobian Matrix} = \frac{\partial L_i(\hat{u}_i)}{\partial s_j} = -B\left(\hat{u}_i, \hat{v}_i, \frac{\partial h(s)}{\partial s_j}\right)$$

inversion problems

Jacobian Function: One TX, one RX

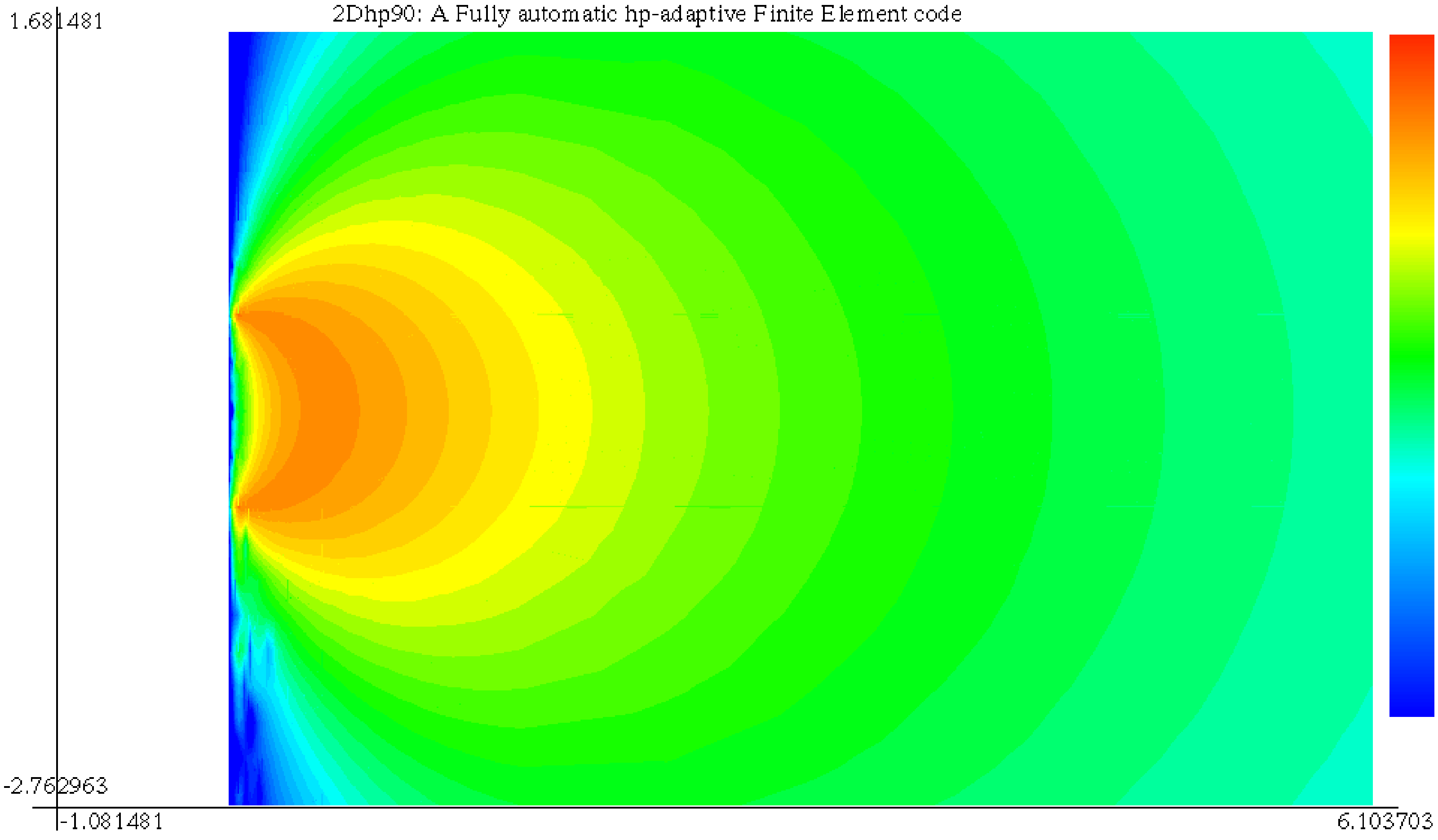

inversion problems

Jacobian Function: One TX, one RX

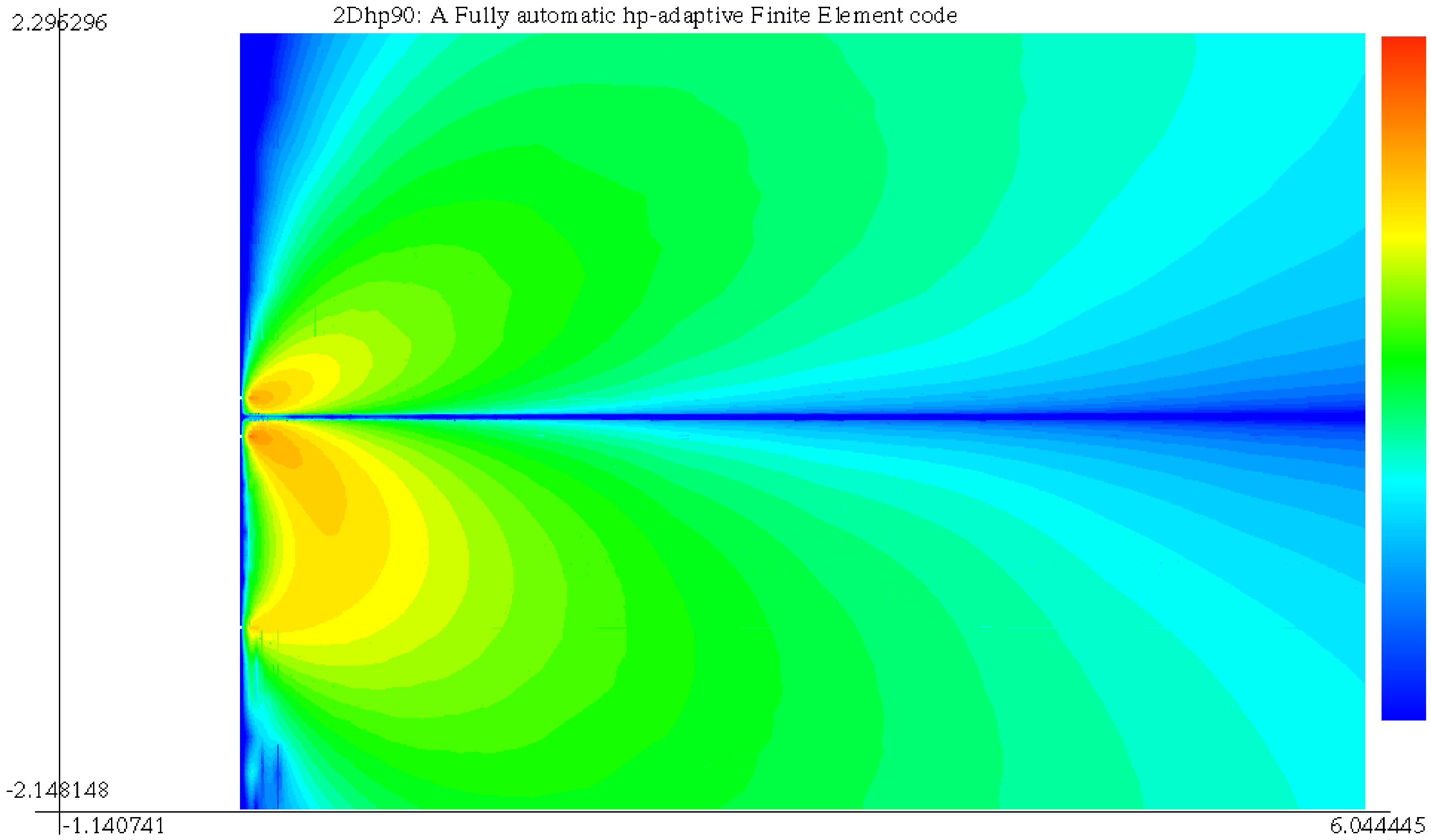

inversion problems

Jacobian Function: One TX, one RX

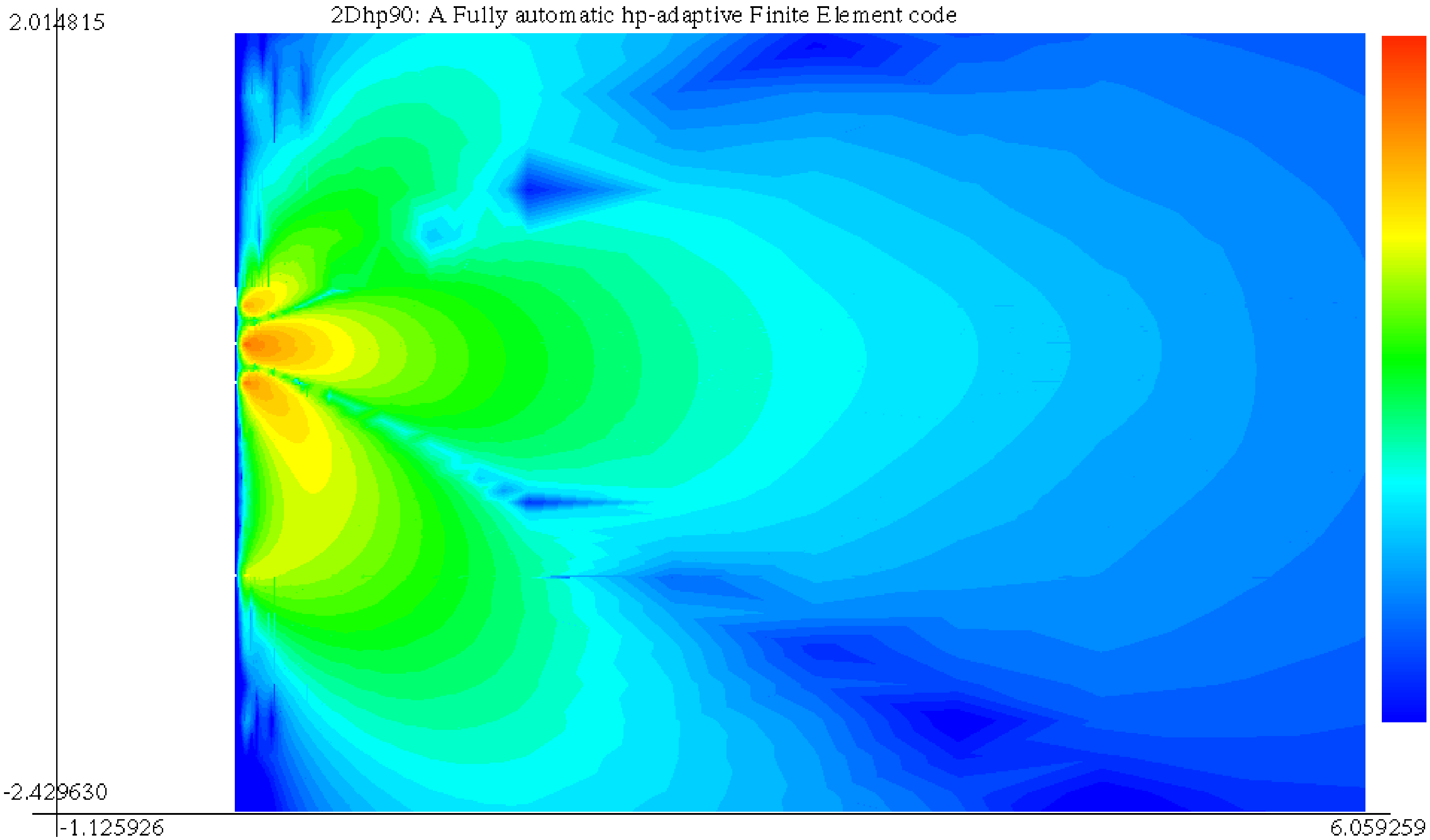

inversion problems

Computation of Hessian Matrix

Following a similar argument as for the Jacobian matrix, we obtain:

$$\frac{\partial^2 L_i(\hat{u}_i)}{\partial s_j \partial s_k} = -B\left(\frac{\partial \hat{u}_i}{\partial s_j}, \hat{v}_i, \frac{\partial h(s)}{\partial s_k}\right) - B\left(\hat{u}_i, \frac{\partial \hat{v}_i}{\partial s_j}, \frac{\partial h(s)}{\partial s_k}\right) - B\left(\hat{u}_i, \hat{v}_i, \frac{\partial^2 h(s)}{\partial s_j \partial s_k}\right)$$

How do we compute $\frac{\partial \hat{u}_i}{\partial s_j}$ and $\frac{\partial \hat{v}_i}{\partial s_j}$?

Find $\frac{\partial \hat{u}_i}{\partial s_j}$ **such that :** $B\left(\frac{\partial \hat{u}_i}{\partial s_j}, v_i, h(s)\right) = -B\left(\hat{u}_i, v_i, \frac{\partial h(s)}{\partial s_j}\right) \quad \forall v_i$

Find $\frac{\partial \hat{v}_i}{\partial s_j}$ **such that :** $B\left(\frac{\partial \hat{v}_i}{\partial s_j}, u_i, h(s)\right) = -B\left(\hat{v}_i, u_i, \frac{\partial h(s)}{\partial s_j}\right) \quad \forall u_i$

We can compute the Hessian matrix EXACTLY by just solving our original problem for different right-hand-sides, and performing additional integrations.

inversion problems

Hessian Function: One TX, one RX

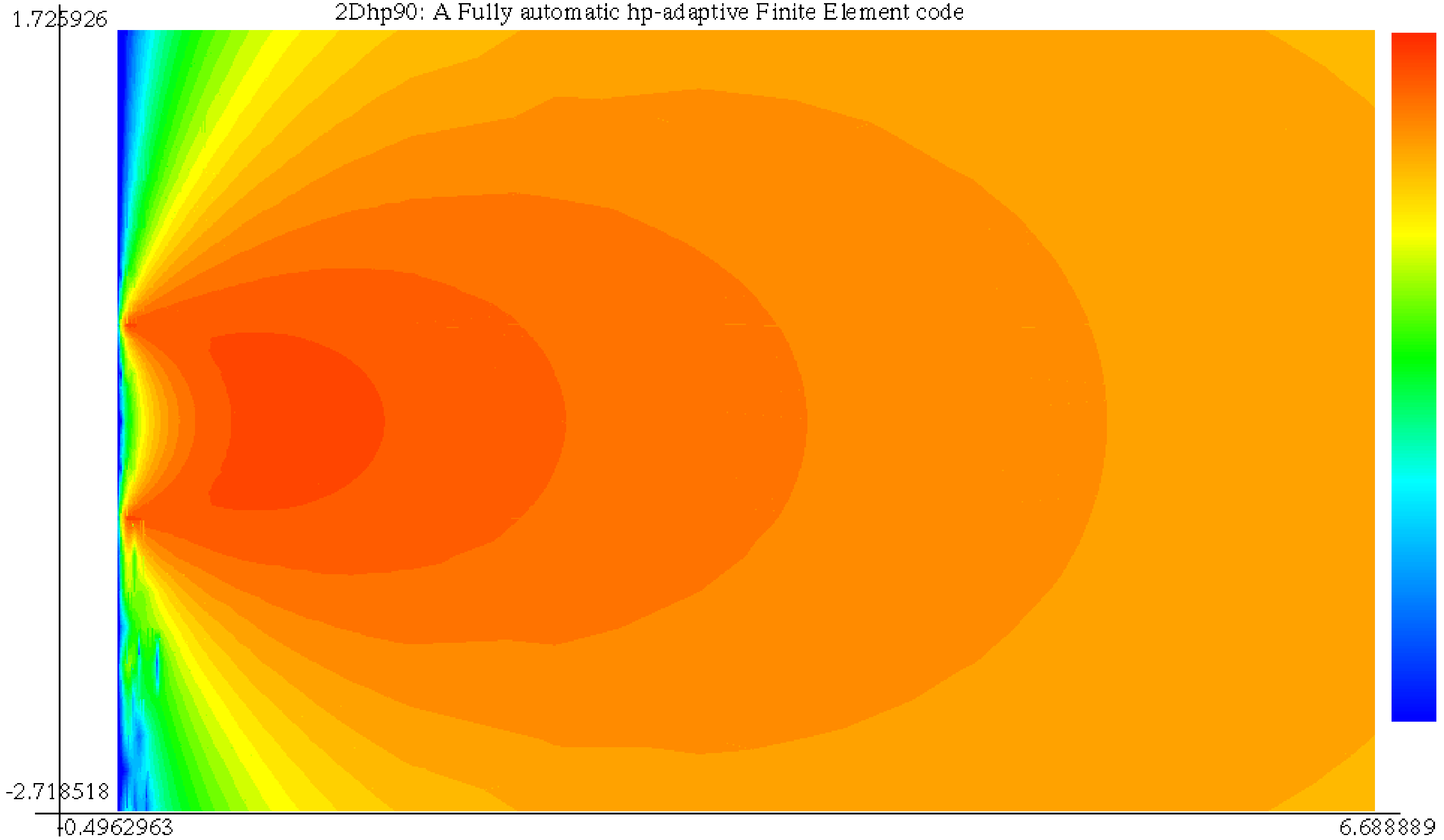

inversion problems

Hessian Function: One TX, two RXs

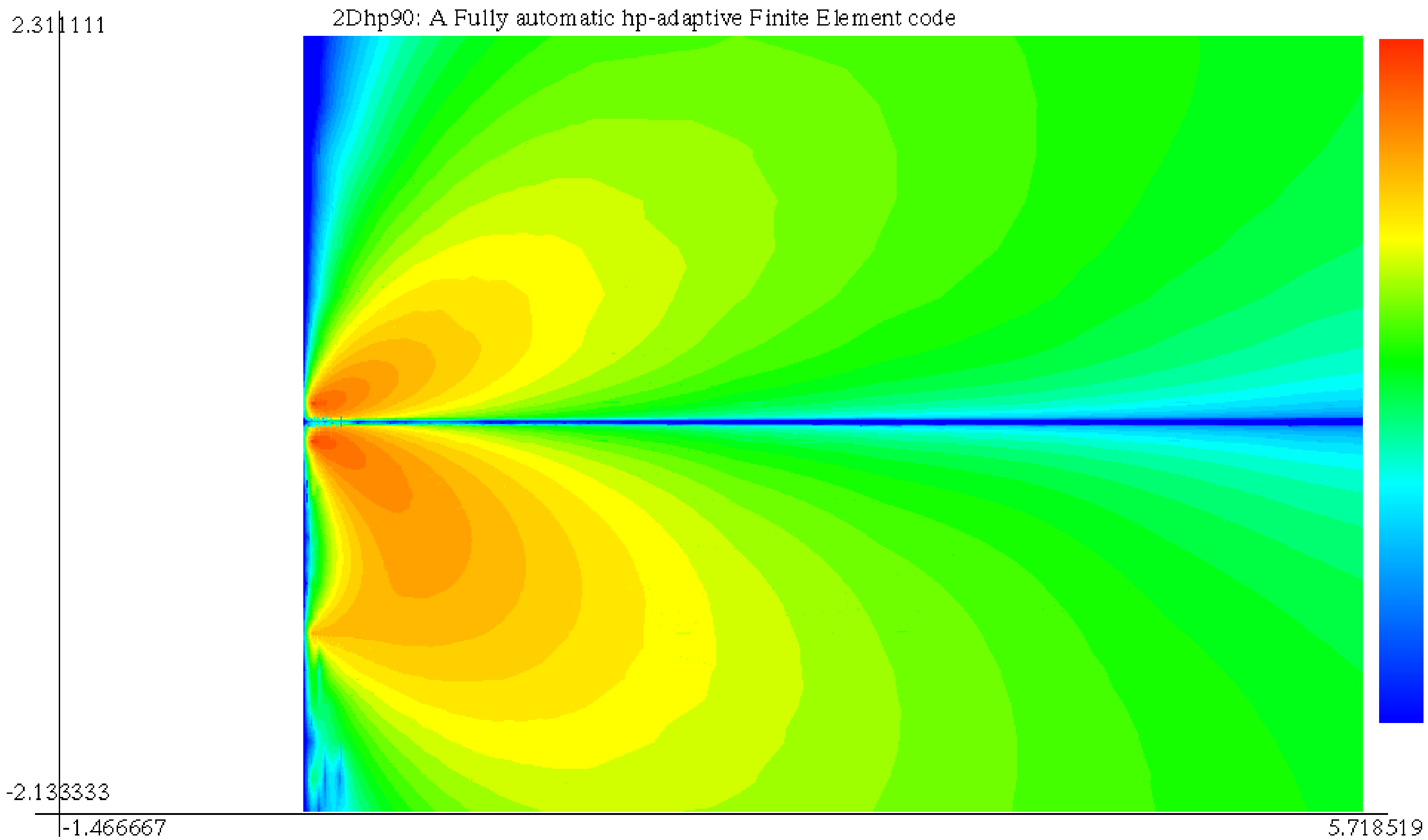

inversion problems

Hessian Function: One TX, three RXs

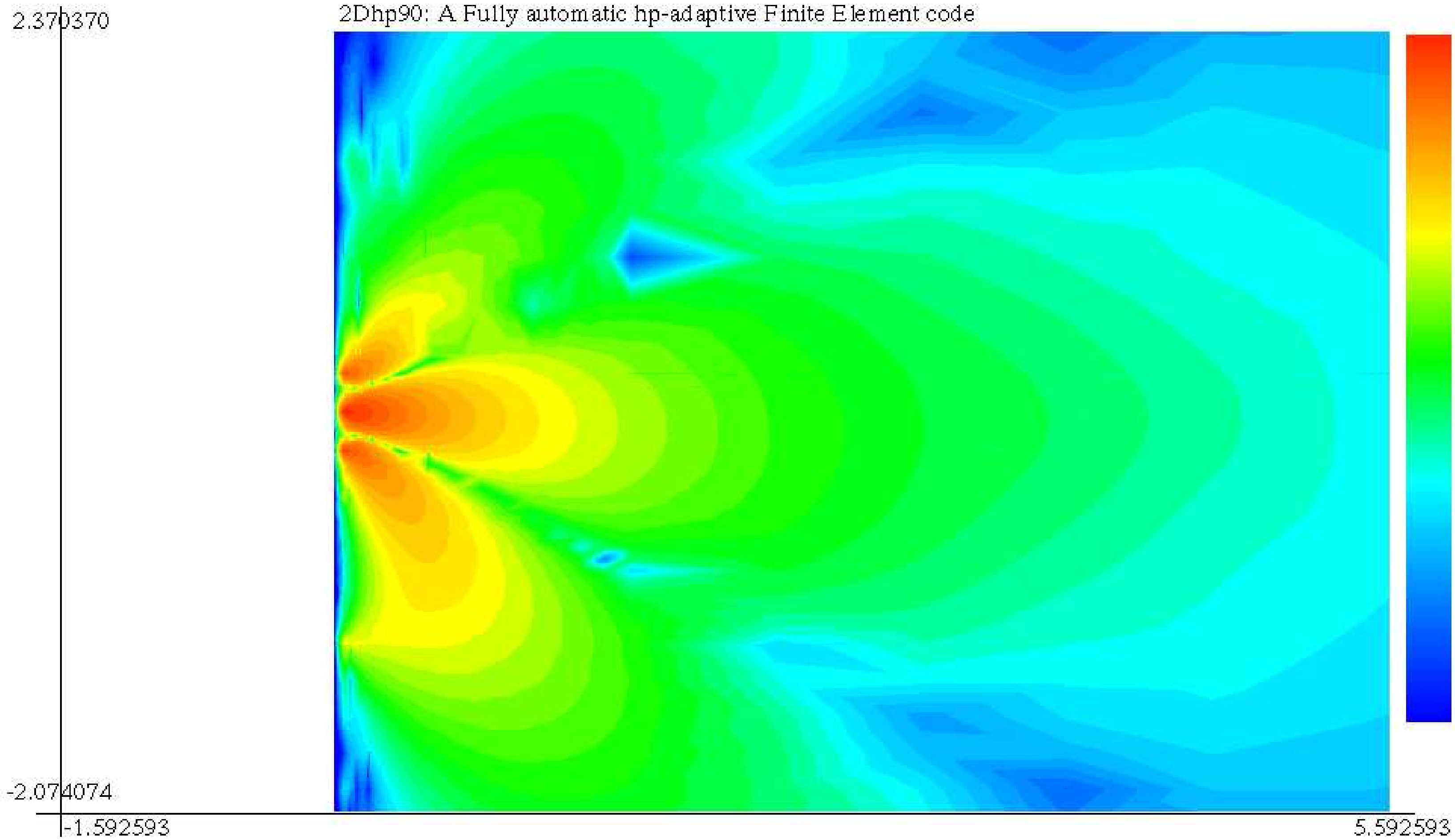

inversion problems

Algorithms implemented within the inverse library

JOINT MULTI−PHYSICS INVERSION LIBRARY

CONSTRAINED OPTIMIZATION	SEARCH DIRECTIONS	STEP SIZE
1. KKT− Conditions	1. Steepest Descent	1. Uniform step−size
2. Penalization Method	2. Gauss−Newton	2. Variable step−size (multiple algorithms)
3. Change of coordinates	3. Newton−Raphson	

The inverse library is composed of multiple algorithms for imposing constraints, and finding search directions and corresponding step sizes.

Jacobian and Hessian matrices are computed exactly by simply solving the dual (adjoint) formulation and performing additional integrations.

The inverse library is compatible with multi-physics problems.

conclusions

- The hp-Finite Element Method provides exponential convergence for a variety of multi-physics problems.
- We succesfully employed a Fourier-Finite-Element method for simulation of electromagnetic and sonic logging measurements.
- We aim to perform joint-inversion of multiphysics measurements with a variety of applications (oil-industry, medicine, etc.).
- We need Ph.D. students, post-doctoral fellows and collaborators in order to solve this and other applications using advanced numerical methods.